

THE FUTURE IMPACTS OF CLIMATE CHANGE ON FISH STOCKS IN THE  
BLACK SEA: AN END-TO-END MODEL APPROACH

A THESIS SUBMITTED TO  
THE GRADUATE SCHOOL OF MARINE SCIENCES  
OF  
MIDDLE EAST TECHNICAL UNIVERSITY

BY

HACER BUSE UYSALER

IN PARTIAL FULFILLMENT OF THE REQUIREMENTS  
FOR  
THE DEGREE OF MASTER OF SCIENCE  
IN  
MARINE BIOLOGY AND FISHERIES

JANUARY 2024



Approval of the thesis:

**THE FUTURE IMPACTS OF CLIMATE CHANGE ON FISH STOCKS IN  
THE BLACK SEA: AN END-TO-END MODEL APPROACH**

submitted by **HACER BUSE UYSALER** in partial fulfillment of the requirements  
for the degree of **Master of Science in Marine Biology and Fisheries, Middle East  
Technical University** by,

Prof. Dr. Barış Salihođlu  
Director, **Institute of Marine Sciences**

\_\_\_\_\_

Prof. Dr. Zahit Uysal  
Head of the Department, **Marine Biology and Fisheries**

\_\_\_\_\_

Assoc. Prof. Dr. Ekin Akođlu  
Supervisor, **Marine Biology and Fisheries, METU**

\_\_\_\_\_

**Examining Committee Members:**

Prof. Dr. Bettina Andrea Fach Salihođlu  
Oceanography, METU

\_\_\_\_\_

Assoc. Prof. Dr. Ekin Akođlu  
Marine Biology and Fisheries, METU

\_\_\_\_\_

Prof. Dr. Nazlı Demirel Erol  
Institute of Marine Sciences and Management, Istanbul  
University

\_\_\_\_\_

Date: 23.01.2024

**I hereby declare that all information in this document has been obtained and presented in accordance with academic rules and ethical conduct. I also declare that, as required by these rules and conduct, I have fully cited and referenced all material and results that are not original to this work.**

Name Last name : Hacer Buse Uysaler

Signature :

## ABSTRACT

### **THE FUTURE IMPACTS OF CLIMATE CHANGE ON FISH STOCKS IN THE BLACK SEA: AN END-TO-END MODEL APPROACH**

Uysaler, Hacer Buse  
Master of Science, Marine Biology and Fisheries  
Supervisor : Assoc. Prof. Dr. Ekin Akođlu

January 2024, 99 pages

The warming of the Black Sea significantly affects the marine ecosystem, fish populations, and livelihoods. Comprehensive models that make assessments about the past, present, and predictions concerning future changes of marine ecosystems are critical tools to better understand marine ecosystem dynamics in response to environmental changes. Until now, the long-term effects of climate change on the Black Sea ecosystem and fish populations have not been extensively studied. This study used the individual-based model OSMOSE (Object-oriented Simulator of Marine Ecosystems Exploitation) to investigate the possible future changes in Black Sea fish stocks under climate change until the end of the 21st century by capitalizing on IPCC climate projections. The dynamics of eight commercially important fish species, anchovy, sprat, Mediterranean horse mackerel, whiting, red mullet, turbot, bluefish, and bonito, were examined under two scenarios, i) a hindcast scenario for 2000-2014, and ii) a future scenario for 2086-2100. The model outcomes showed consistent alignment with observed data. The model results showed that there will be an increase in biomass and catch values of all fish species, as a result of predicted increases at lower trophic levels. Furthermore, predicted increases were generally

observed for all size classes. Smaller individuals were projected to dominate the system, demonstrating the impact of unsustainable fishing. The findings of this study could provide critical insights for the development of climate-adapted fishing strategies in the Black Sea using a size-based opportunistic predation approach. Therefore, these strategies should focus on the recovery of populations in larger size classes, with climate-adapted strategies to ensure sustainable and long-term fisheries.

Keywords: Black Sea, Fish Stocks, Ecosystem Modelling, Climate Change, Fisheries

## ÖZ

### İKLİM DEĞİŞİKLİĞİNİN KARADENİZ BALIK STOKLARINA GELECEKTEKİ ETKİLERİ: BAŞTAN SONA BİR MODEL YAKLAŞIMI

Uysaler, Hacer Buse  
Yüksek Lisans, Deniz Biyolojisi ve Balıkçılık  
Tez Yöneticisi: Assoc. Prof. Dr. Ekin Akoğlu

Ocak 2024, 99 sayfa

Karadeniz'in ısınması deniz ekosistemini, balık popülasyonlarını ve bu popülasyonların etkilediği geçim kaynaklarını önemli ölçüde etkilemektedir. Deniz ekosisteminin çevresel değişikliklere verdiği tepkileri daha iyi anlamak adına, ekosistemin geçmişi, bugünü ve geleceği hakkında tahminler veren detaylı modeller kritik önem taşımaktadır. Şimdiye kadar, iklim değişikliğinin Karadeniz ekosistemi ve balık popülasyonları üzerindeki uzun vadeli etkileri kapsamlı olarak incelenmemiştir. Bu çalışmada, 21. yüzyılın sonuna kadar IPCC iklim değişikliği senaryoları altında Karadeniz balık stoklarındaki olası gelecekteki değişikliklerini değerlendiren bireye dayalı OSMOSE (Object-oriented Simulator of Marine Ecosystems Exploitation) modeli kullanılmıştır. Hamsi, çaça, istavrit, barbun, mezigit, kalkan, lüfer ve palamut olmak üzere ticari açıdan önemli sekiz balık türünün dinamikleri, 2000-2014 için bir güncel durum senaryosu ve 2086-2100 için bir gelecek senaryosu altında incelenmiştir. Model sonuçları gözlemlenen verilerle tutarlılık elde etmiştir. Sonuçlar, tüm balık türlerinin popülasyonlarında ve av değerlerinde, alt trofik seviyelerdeki artışlarla ilişkili olarak bir artış olacağını öngörmüştür. Bu artışlar bütün türler için tüm boy sınıflarında gözlemlenmiştir. Daha küçük bireylerin sisteme hakim olacağı öngörülmüş ve bu da sürdürülebilir

olmayan balıkçılığın etkisini göstermiştir. Bu çalışmanın bulguları, boyuta dayalı fırsatçı avlanma yaklaşımını kullanarak Karadeniz'de iklime uyumlu balıkçılık stratejilerinin geliştirilmesine yönelik kritik bilgiler sağlayabilir. Bu stratejiler, sürdürülebilir ve uzun vadeli balıkçılık sağlamak için iklime uyumlu stratejilerle birlikte, daha büyük boy sınıflarındaki balık popülasyonlarının toparlanmasına odaklanmalıdır.

Anahtar Kelimeler: Karadeniz, Balık Stokları, Ekosistem Modellemesi, İklim Değişikliği, Balıkçılık



To all the fighting spirits whose journey is paved with love

To my family & Suki

## ACKNOWLEDGMENTS

First and foremost, I am profoundly thankful to my supervisor, Assoc. Prof. Dr. Ekin Akođlu, for his guidance, advice, criticism, and encouragement. He always believed in and supported me, even in the most chaotic situations. I am deeply grateful to have started my journey in marine sciences under his supervision.

I extend my sincere appreciation to the members of my thesis committee, Prof. Dr. Bettina Andrea Fach Salihođlu and Prof. Dr. Nazlı Demirel Erol, for their support and contribution to this study.

I am grateful to Ricardo Oliveros-Ramos, Yunne-Jai Shin, and Nicolas Barrier for providing access to their DATARMOR computing resources (<http://www.ifremer.fr/pcdm>) and for their guidance with the OSMOSE model code.

I would like to express my sincere thanks to the academic and administrative people at METU, the Institute of Marine Sciences. I am especially thankful to Gizem Akkuş, Merve Kurt, Nimet Alımlı, Begüm Ece Tohumcu, Suna Tüzün, Burak Kuyumcu, and Serhat Sevgen for their friendship, support, and helpful answers in this field.

I wish to thank İrem Yeşim Savaş, Hasan Arslan, and Polen Alemdar for their support and help during challenging times in the last few months.

I offer my heartfelt thanks to every member of Setüstü for their support, providing delicious food and care when I had to study for hours. Your friendships and shared experiences have made this journey memorable. Special thanks to Deniz Eşkinat, Emel Kocaman, and Serhat Ertuđrul for their friendship during this journey.

I am very grateful to Onur Karakuş for his camaraderie, encouragement, and endless support whenever I needed it. I extend my sincere gratitude to Ehsan Sadighrad for his valuable guidance, friendship, and unwavering support.

I would like to thank my friends Merve Timurođulları, Elif Yapıcı, Dudu Erol, Zeynep Abalı, Alişan Kayabölen, and many others who have always stood by me for their significant contributions and motivations in my life for almost a decade.

I owe the deepest gratitude to my father Ömer Uysaler, my mother Aslıhan Uysaler, my sister Sude Uysaler, my grandmother Hülya Türkgüler, and the rest of my family for their love and all the sacrifices they have made. They have always believed in and supported me in all my decisions throughout the years. Lastly, I thank Suki for enabling me to explore a spectrum of emotions and enriching my life with its presence.

This study was supported by the Scientific and Technological Research Council of Türkiye under grant number 218Z151, METU, and the SOMBEE project of the joint BiodivERsA and Belmont Forum.

## TABLE OF CONTENTS

ABSTRACT .....	v
ÖZ .....	vii
ACKNOWLEDGMENTS .....	x
TABLE OF CONTENTS .....	xii
LIST OF TABLES .....	xiv
LIST OF FIGURES .....	xv
CHAPTERS	
1 INTRODUCTION .....	1
1.1 Study Objectives.....	6
2 MATERIAL AND METHOD.....	7
2.1 The Study Area.....	7
2.2 The Modelling Approach: OSMOSE-BS .....	10
2.2.1 Scenarios.....	12
2.2.2 Low Trophic Levels from IPSL-CM6A-LR.....	12
2.2.3 High Trophic Levels .....	13
2.3 Calibration of OSMOSE-BS .....	25
2.4 Model Validation.....	26
2.5 Analysis of the OSMOSE-BS's Results.....	27
3 RESULTS.....	29
3.1 Current and Future IPSL-CM6A-LR Projections.....	29

3.2	Hindcast Simulation, Model Validation and Skill .....	32
3.3	Forecast Simulation .....	36
3.3.1	The Comparison Between Forecast and Hindcast Scenarios .....	40
3.4	Spatial Distributions.....	50
4	DISCUSSION .....	55
4.1	Model Representation .....	55
4.2	Model Validation and Skills .....	57
4.3	Evaluation of Model Results.....	59
4.4	Limitations and Future Work.....	62
4.5	Potential uses of OSMOSE-BS.....	64
5	CONCLUSION.....	67
	REFERENCES .....	69
	APPENDICES	
A.	OSMOSE-BS Parameters .....	89
B.	OSMOSE-BS Results .....	96
C.	Lower Trophic Level Changes.....	99

## LIST OF TABLES

### TABLES

Table 1 Parametrization of the LTL .....	13
Table 2. Growth and reproduction parameters of OSMOSE-BS for eight HTL species. $L_{\infty}$ , $K$ , and $t_0$ are the von Bertalanffy growth parameters; $c$ is Fulton's condition factor, and $b$ is the exponent of the length-weight (L-W) allometric relationship. <i>Ratiosex</i> is the ratio females to males in the population. $\Phi_s$ is the relative fecundity, <i>Lmat</i> represents the length at first maturity.....	20
Table 3. Mortality parameters of OSMOSE-BS for eight HTL species. <i>MF</i> , <i>MN</i> and <i>Mout</i> are fishing, natural and migration mortality rates, respectively. <i>Rmax</i> and <i>Rmin</i> are maximum and minimum predator/prey size ratio.....	22
Table 4. Accessibility matrix for anchovy(sp0), sprat(sp1), Med. horse mackerel (sp2), red mullet(sp3), whiting (sp4), turbot (sp5), bluefish (sp6), and bonito (sp7).....	22
Table 5. Migration season and ages for anchovy, bluefish, and bonito .....	23
Table 6. Recruitment sizes that were manually tuned after the calibration.....	26
Table 7. Calibration parameters of OSMOSE-BS.....	32
Table 8. The centered root mean square error.....	33

## LIST OF FIGURES

### FIGURES

Figure 1. The history of the ecosystem changes in the Black Sea (Akoglu et al., 2014) .....	5
Figure 2. The Black Sea .....	8
Figure 3. The surface circulation patterns of the Black Sea (Oguz et al., 2005) .....	9
Figure 4. Conceptual representation of the OSMOSE-BS end-to-end model. The OSMOSE model was forced by the IPSL-CM6A-LR model through the predation of fish species on lower trophic levels. ....	11
Figure 5. Reproduction seasonality for eight HTL groups. ....	21
Figure 6. Prescribed spatial distributions, i.e., most likely occurrence, of HTL species in the OSMOSE-BS model.....	24
Figure 7. Annually-averaged time series of sea surface temperature for hindcast and forecast scenarios. ....	30
Figure 8. Annually-averaged time series of biomass of mesozooplankton (Zo), microzooplankton (Zm), detritus (Dn) in hindcast (left) and forecast (right) scenarios.....	31
Figure 9. Annually-averaged time series of vertically-integrated primary production in hindcast (left) and forecast (right) scenarios.....	31
Figure 10. The comparison of simulated biomasses of six HTL species against stock assessment estimated biomasses over a 15-year hindcast simulation. The gray-shaded bands represent the maximum and minimum intervals obtained from 10 simulation replicates. The dots represent the stock assessment estimated biomasses. ....	34
Figure 11. The comparison of simulated catches of eight HTL species against statistical catch data over a 15-year hindcast simulation. The gray-shaded bands represent the maximum and minimum intervals obtained from 10 simulation replicates. The dots represent the statistical catches. ....	35

Figure 12. The mean size at catch for eight HTL species over the 15-year hindcast simulation. The vertical red bars correspond to the standard deviation of the simulations across 10 replicates. The black diamonds represent the observed sizes. .... 36

Figure 13. The mean biomass values predicted by OSMOSE-BS for the eight fish species during 2086-2100. The gray-shaded area represents the maximum and minimum intervals obtained from 10 simulation replicates. .... 38

Figure 14. The mean catch values predicted by OSMOSE-BS of the eight fish species during 2086-2100. The gray-shaded area represents the maximum and minimum intervals obtained from 10 simulation replicates. .... 39

Figure 15. The mean size at catch in forecast scenario for the eight fish species during 2086-2100. The vertical red bars correspond to the standard deviation of the simulation across 10 simulation replicates. The black diamonds represent the observed sizes. .... 40

Figure 16. Fractional change in biomass of LTL species between forecast and hindcast scenarios. .... 41

Figure 17. Fractional change in biomass and catch between forecast and hindcast scenarios. .... 42

Figure 18. Fractional change in mean size of catch between forecast and hindcast scenarios. .... 43

Figure 19. Fractional change of biomass distribution by size between forecast and hindcast scenarios for the small pelagic species' populations. .... 44

Figure 20. Fractional change of biomass distribution by size between forecast and hindcast scenarios for the demersal pelagic species' populations. .... 45

Figure 21. Fractional change of biomass distribution by size between forecast and hindcast scenarios for the large pelagic species' populations. .... 45

Figure 22. Proportions of the biomasses in size classes to the total biomasses of anchovy, sprat, and horse mackerel over 15 years within different size-classes for hindcast (2000–2014, light-gray bars) and forecast (2086–2100, dark-gray bars) scenarios. .... 47



Figure 23 Proportions of the biomasses in size classes to the total biomasses of red mullet, whiting and turbot over 15 years within different size-classes for hindcast (2000–2014, light-gray bars) and forecast (2086–2100, dark-gray bars) scenarios. ....	48
Figure 24 Proportions of biomasses in size classes to the total biomass of bluefish and bonito over 15 years within different size-classes for hindcast (2000–2014, light-gray bars) and forecast (2086–2100, dark-gray bars) scenarios.....	49
Figure 25. Proportions of biomasses in size classes to the total biomasses over 15 years within different size-classes for hindcast (2000–2014, light-gray bars) and forecast (2086–2100, dark-gray bars) scenarios. ....	50
Figure 26. The spatial distribution of average biomass obtained from 10 simulation replicates for the hindcast scenario. ....	52
Figure 27. The spatial distribution of average biomass obtained from 10 simulation replicates for the forecast scenario. ....	53
Figure 28. The change in spatial distribution of average biomass between the hindcast and forecast scenarios. ....	54
Figure 29. Median biomass values in the 2000–2014 period for OSMOSE-BS and EwE (Salihoğlu et al., 2017). ....	56
Figure 30. Schematic diagram of food web diet representations for OSMOSE-BS and EwE (adapted from Salihoğlu et al., 2017). The arrow represents the flow of prey-predator interactions. Zo and Zm represent mesozooplankton and microzooplankton, respectively. The model groups shown in EwE were selected to correspond to species in OSMOSE. ....	57



## **CHAPTER 1**

### **INTRODUCTION**

The oceans, which cover approximately 71% of the world, play a pivotal role in advancing life on our planet and regulating global climate patterns (Hoegh-Guldberg et al., 2019). The oceans' crucial influence on planetary mechanisms includes carbon cycling, carbon dioxide sequestration, and accounting for half of the planet's primary production (Brierley & Kingsford, 2009; Hoegh-Guldberg et al., 2014). Furthermore, the abundance of marine fish and their byproducts, which include fishmeal, fish oil, and baits, as well as sources of pharmaceuticals and cosmetics, constitute an essential component of sustenance and income for people (FAO, 2014). However, marine ecosystems and species that depend on them currently face climate change, one of the most significant anthropogenically-driven environmental challenges, resulting in increasing global temperatures, altered precipitation patterns, and a rise in the frequency of extreme weather events (IPCC, 2007). These effects are further compounded by subsequent increases in ocean temperatures, acidification, altered ocean circulation, and concurrent deoxygenation, making them major stressors affecting ocean ecosystems (Gruber, 2011; Hoegh-Guldberg et al., 2014; Keeling et al., 2010; Pörtner et al., 2014). Alongside climate change, overfishing and unsustainable fishing techniques have widespread negative impacts on marine ecosystems and pose conservation risks to numerous marine species. The ratio of fish stocks that are being exploited at unsustainable levels has increased from 10% to 35.4% since the 1970s (FAO, 2022). Therefore, decreases in fish biomass, destruction of marine habitats due to destructive fishing gears such as dredges and bottom trawls, alterations in biodiversity composition, and regime shifts (Pauly et

al., 2005; Sumaila & Tai, 2020) have become widespread phenomena in marine ecosystems.

The impact of climate change profoundly influenced marine ecosystems, from primary producers to top predators. These changes had direct and indirect consequences on high trophic level species, encompassing modifications in fish population dynamics, spatial distribution, and life-history attributes. Temperature fluctuations may change the physiological responses of organisms, resulting in changes in their biological performance, such as metabolic rates, growth, reproduction, and survival (Stenseth et al., 2002; Sumaila & Tai, 2020). Alterations in vertical stratification and mixing affect nutrient cycling, primary production, and plankton biomass (Chust et al., 2014; Oguz, 2005). Garrabau et al. (2009) indicated mass mortality in benthic communities associated with temperature alterations in the Northwestern Mediterranean Sea. Köster et al. (2005) investigated the impacts of climate variations and found that a decrease in salinity and oxygen concentrations resulted in egg mortalities of the eastern Baltic cod in the Baltic Sea. Chavez et al. (2003) observed that anchovy decreases were linked to warming effects on productivity, while sardines tended to increase in the Pacific Ocean.

As climate change affected fish populations, fisheries were consequently impacted, and appropriate fisheries management policies must be implemented considering the climate variations (Gaines et al., 2018). Furthermore, excessive, and illegal fishing exacerbated these effects even further (Öztürk, 2013). Reduction of larger and more valuable fish species results in fishing down in the food webs (Pauly et al., 2005), that is the disappearance of larger individuals in fish populations, making smaller and less valuable fishes dominant in the ecosystem. According to Perry et al. (2010), these changes on marine fish populations led to increases in their sensitivity to environmental stressors such as climate change. Therefore, it is essential to consider the combined effects of climate change and overfishing on marine fish populations.

Climate change impose significant direct and indirect shifts in marine ecosystems; therefore, understanding the intricate interplays between biodiversity and trophic

relationships becomes crucial. The development of comprehensive models is crucial for accurately capturing the complex interactions of the food web, from the bottom to the top (Travers et al., 2007). In this context, end-to-end models (E2E) were considered appropriate tools to represent the whole ecological system, integrating both biotic and abiotic components (Fulton, 2010). The combined effects of fisheries and climate change need to be considered simultaneously to achieve more reliable analyses and predictions in marine ecosystem dynamics (Travers et al., 2007). This importance has led to the development of models such as OSMOSE (Shin & Cury, 2001, 2004), Ecopath with Ecosim (Christensen & Walters, 2004), Atlantis (Fulton et al., 2005), SEAPODYM (Lehodey et al., 2003; Lehodey, 2005), and APECOSM (Maury et al., 2007). These models also consider the question from a fisheries aspect and the integrated impacts of climate variations and overfishing (Travers-Trolet et al., 2014).

End-to-end models can be established by coupling existing models: physical models with the abiotic conditions, biogeochemical models representing nutrient and plankton dynamics, and higher trophic level models (Cury et al., 2008). The coupling procedure is enabled by information transfer between models: the output component of one model provides input to the other model. The link between the lower-trophic-level (LTL) model to higher-trophic-level (HTL) model is usually through predation. This linking process impacts both the growth rate of predators and the mortality of the prey (Cury et al., 2008; Travers et al., 2007).

Being some of the most anthropogenically and climate change-affected areas, marginal seas provide valuable opportunities for studies aiming to understand effects of climate change on marine ecosystems (Oguz et al., 2006). The Black Sea holds particular interest due to a combination of factors such as intense eutrophication, overfishing, and population outbreaks of indigenous species, as well as the influence of climate-induced variations on these conditions (Daskalov, 2003; Oguz, 2005; Zaitsev & Mamaev, 1997). Considering fish stocks, the Black Sea is one of the areas at risk from overfishing. Previous studies revealed that 85% of fish stocks in the Black Sea have been overexploited (Daskalov, 2002; Sherman & Adams, 2010;

Demirel et al., 2020). Given its unique characteristics and ecological importance, the Black Sea serves as an excellent case study among the marginal seas for examining the impacts of climate change on fish stocks.

The Black Sea ecosystem has experienced significant ecological changes since the latter half of the 20th century. These dramatic changes were brought about by the combined effects of eutrophication, overfishing, population outbursts of non-indigenous species (Gucu, 2002; Kideys, 2002; Zaitsev & Mamaev, 1997) in addition to climate-driven fluctuations (Daskalov, 2003; Oguz, 2005). During the 1970s and 1980s, excessive riverine nutrient enrichment into the northwestern shelf caused severe eutrophication that resulted in hypoxia following the deterioration of benthic habitat (Zaitsev & Mamaev, 1997). Concurrently, this was accompanied by intense fishing pressure, leading to a reduction in medium and large pelagic fish stocks. This contributed to the dominance of smaller planktivorous fish, primarily anchovy and sprat, which became the main interest of fishing within the ecosystem (Oguz, 2005). At the same time, the population of *Aurelia aurita* (Linnaeus, 1758) increased in the system, potentially due to a decrease in its predator pressure, the overexploitation of Atlantic mackerel (Arai, 2001), and eutrophication (Caddy & Griffiths, 1990). In the late 1980s, *Aurelia aurita* reached its highest value (Oguz, 2005), coinciding with the population explosion of the non-indigenous *Mnemiopsis*, which was introduced to the Black Sea in the early 1980s through ballast waters. This period also witnessed the significant collapse of small and medium pelagic fisheries (Oguz, 2007), and the decline of anchovy population, which was dominant in the early 1980s (Ivana & Panayotova, 2001). Thereupon, the collapse of fisheries, particularly the Turkish fishery yield, lasted until 1993, after which it began to gradually recover (Oguz et al., 2012). Towards the end of the 1990s, the level of primary and secondary productivity in the Black Sea ecosystem was moderate (Mee, 2006; Oguz et al., 2012), while the stocks of both plankton and fish showed ongoing fluctuations (Figure 1).

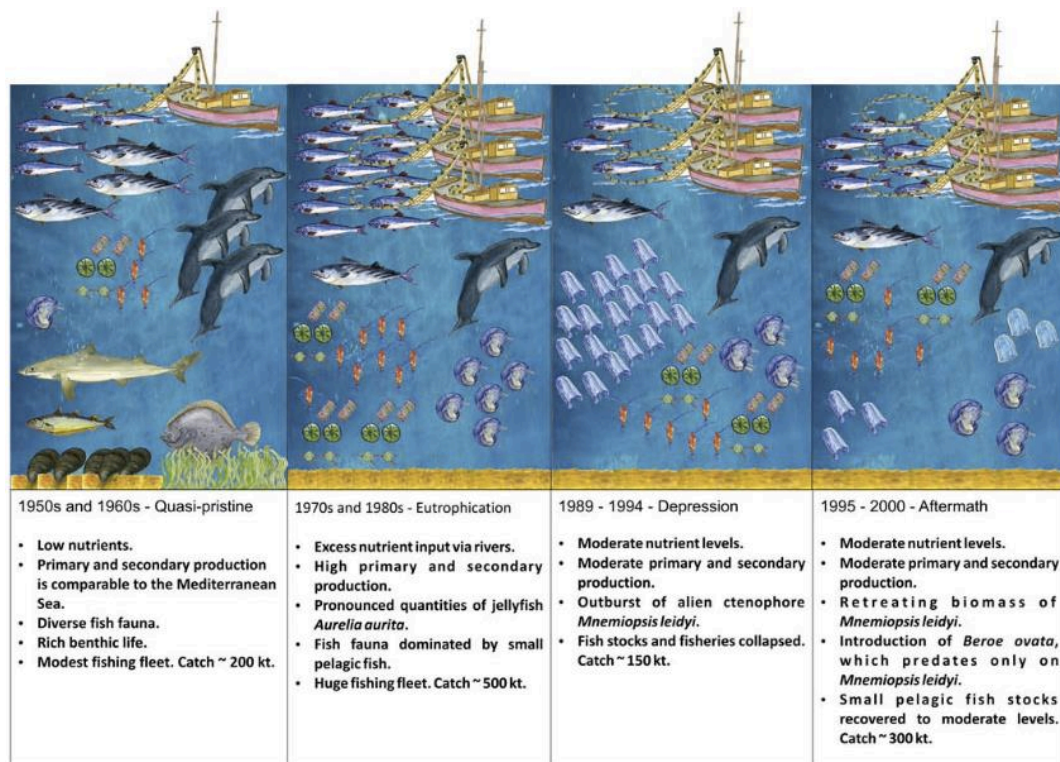


Figure 1. The history of the ecosystem changes in the Black Sea (Akoglu et al., 2014)

In order to better understand ecosystem changes and dynamics in the Black Sea, various mass-balance models and the examination of long-term time-series data have been applied. Overfishing or trophic cascades caused by overfishing were associated with a decline in anchovy populations (Daskalov, 2002; Gucu, 2002). Akoglu et al. (2014) investigated ecosystem food web structure through regime shifts using indicator-based analysis of the combined effects of anthropogenic and natural stressors in the Black Sea and found eutrophication and overfishing to be primary factors responsible for the different regimes in the Black Sea in 1960–2000 (Akoglu, 2023). In addition to examining ecosystem changes in the last half of the 20th century, Salihoglu et al. (2017) showed that alterations in planktonic production directly affected small pelagic fish, even in the presence of intense fishing activities after the 2000s. Overall, ecological modelling studies in the Black Sea aimed to understand significant ecosystem changes and the reasons behind them; however,

predicting how fish dynamics will change with a focus on future climate change is still a gap in knowledge.

## **1.1 Study Objectives**

The principal objective of this study is to deepen our understanding of how future climate variations might impact eight economically crucial fish species in the Black Sea by implementing an individual-based model with sized-based opportunistic predation approach for the Black Sea ecosystem for the first time. Considering the economic and sociological importance of Black Sea fisheries, the insights gained may guide future evolution of fishing management and size-based strategies.

Within the scope of these broad aims, I sought answers to the following research questions:

- i) How can a representation of the Black Sea ecosystem using sized-based opportunistic predation approach differ compared to earlier modelling studies, and what kind of improvements such an implementation may provide for the assessment of the dynamics of the fish stocks in the Black Sea?
- ii) How can the dynamics of eight commercially-exploited fish populations change under the impact of climate change by the end of this century?
- iii) What kind of mitigation strategies could be required to sustainably manage fish stocks in the Black Sea by comparing the current and future climate projections for changes in the fish populations based on biomass, catch, and size over time?



## **CHAPTER 2**

### **MATERIAL AND METHOD**

#### **2.1 The Study Area**

The Black Sea is located within the geographical coordinates between latitudes 41° to 46°N and longitudes 28° to 41.5°E approximately. It is located between Europe and Asia and surrounded by six countries, namely Ukraine, Russia, Georgia, Türkiye, Bulgaria, and Romania (Figure 2). The surface area of the Black Sea without the Sea of Azov spans 423,000 km<sup>2</sup>, and it holds a total volume of 547,000 km<sup>3</sup>. Its maximum depth reaches 2,212 m (Zaitsev & Mamaev, 1997).

The Black Sea, one of the largest semi-enclosed basins globally, has limited connectivity with the ocean. To the north, it is connected to the Sea of Azov via the Kerch Strait, while in the southwest, it is linked to the Mediterranean Sea through the Bosphorus Strait, followed by the Sea of Marmara and the Dardanelles Strait.

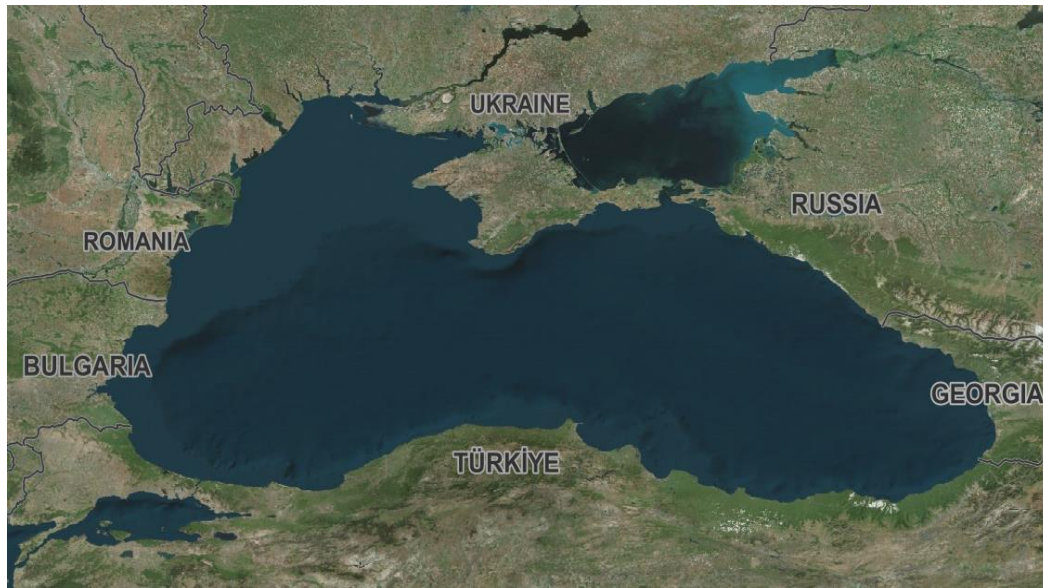


Figure 2. The Black Sea

The Black Sea exhibits a significantly lower salinity in its surface layer in comparison to the other seas due to the high level of river input in the upper layer (Konovalov et al., 2005). The Black Sea receives discharges from Europe's big rivers such as the Danube, the Dniester, the Dnieper, South Bug, sustaining the low salinity on the surface. The only source of salty water coming to the Black Sea is the Mediterranean water entering through the Bosphorus Strait. This ensures a vertical stratification as a result of strong density difference. The surface layer of the Black Sea is rich in oxygen, whereas the deep layer ( $> \sim 150$  m) is devoid of oxygen and has high levels of sulfide. The suboxic zone, between the oxic surface layer and anoxic deeper layers, has a remarkably low concentration of  $O_2$  and  $H_2S$  (Murray et al., 1989).

The considerable difference in salinity levels within the Black Sea water column results in the formation of a two-layered system characterized by restricted mixing, due to the presence of a persistent halocline. In the winter months, the cooling surface water mass descends and establishes a cold intermediate layer (CIL) with temperatures ranging from 6-8 °C, situated between the seasonal thermocline and the halocline. As the spring and summer months progress, the CIL becomes more

pronounced as a result of the increased warming of the surface water (Oguz et al., 1992). However, the temperature of this layer approached around 9 °C in recent years as a result of climate change, indicating a state of disappearance (Stanev et al., 2019).

The surface waters in the Black Sea are controlled by the circulation patterns depicted in Figure 3. The Black Sea has two-gyre structures in each eastern and western part covered by a cyclonic Rim Current system, which undergoes seasonal variation. Within the Rim Current and the coastal areas, several anticyclonic eddies also play a role in controlling the upper layer dynamics. The deeper layers are more stable and seasonal variations do not affect the circulation due to density stratification.

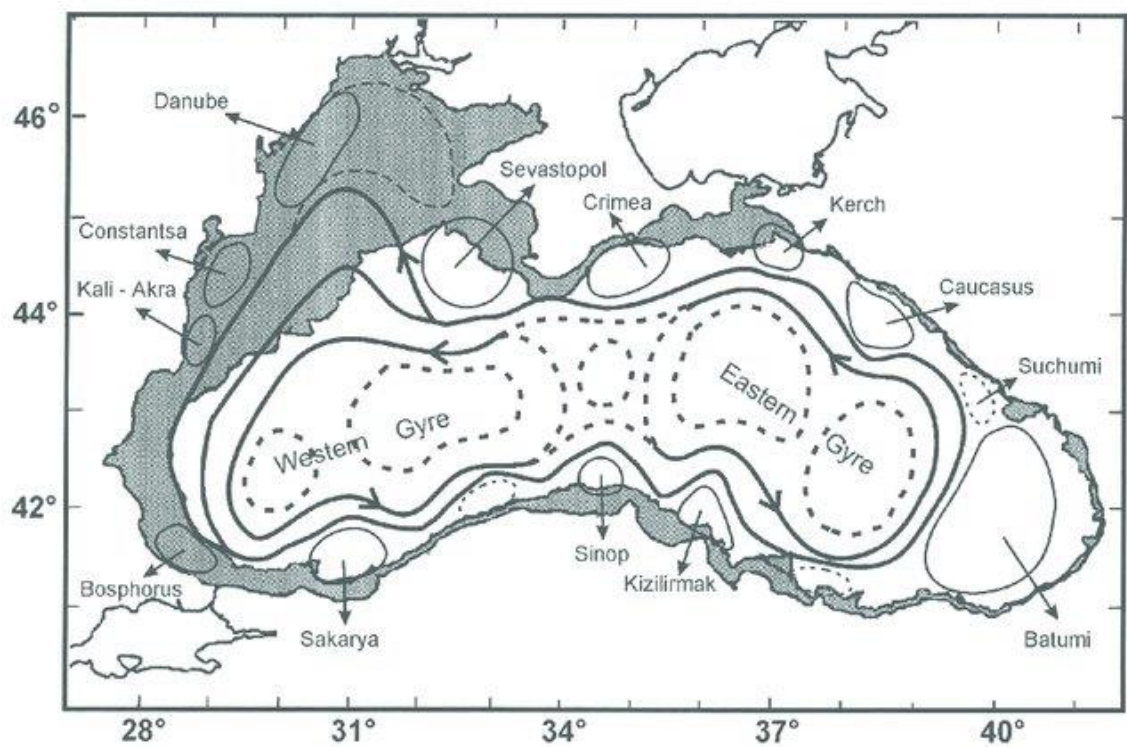


Figure 3. The surface circulation patterns of the Black Sea (Oguz et al., 2005)

According to the Food and Agriculture Organization (FAO), fish stocks in the Mediterranean and Black Sea have been fished at unsustainable levels; in fact, in 2020, 73% of fish stocks were fished beyond biologically sustainable limits. The average landings for the Black Sea during 2018–2020 amounted to 446100 tonnes, which representing a 15% increase compared to the catch from 2016 to 2018. Among the Black Sea countries, Türkiye dominated the catch with 275500 tonnes in 2018–2020. The European anchovy was unquestionably the most predominant species in the Black Sea, accounting for 64.7% of the total landings, followed by sprat at 11.2%. Moreover, Mediterranean horse mackerel and whiting constituted 2.4% and 1.8%, respectively, whereas bluefish comprised 0.8% of the landings (FAO, 2022). Furthermore, many of the target species in the Black Sea have been affected by illegal, unreported, and unregulated (IUU) fishing activities (Öztürk, 2015) and have also been caught as by-catch (Raykov et al., 2008). European anchovy was considered the primary unreported species in terms of tonnage because of its high catch proportion (Ulman et al., 2013).

## **2.2 The Modelling Approach: OSMOSE-BS**

OSMOSE (Object-oriented simulator of marine ecosystems exploitation) is a two-dimensional spatially-explicit, individual-based multispecies model developed by Shin & Cury (2001, 2004). OSMOSE provides trophic interaction simulations of marine nektonic species. The model represents the whole lifecycle of HTL species, (i.e., fish, shellfish and marine molluscs) and does not have the capacity to simulate biogeochemical and lower-trophic-level, i.e., plankton dynamics. Species in the model are represented through physiological processes of growth, predation, reproduction, and mortality throughout their life histories (Shin & Cury, 2004). In this study, the OSMOSE model was implemented specifically for the Black Sea, which was referred to as OSMOSE-BS hereinafter.

OSMOSE end-to-end modelling approach requires that the model is coupled to a biogeochemical model to provide resource forcing such as phytoplankton,

zooplankton, and detritus biomasses. Therefore, LTL input data was obtained from The Institut Pierre-Simon Laplace (IPSL) Low-Resolution (LR) global Climate Model (CM) (IPSL-CM6A-LR) via the Inter-Sectoral Impact Model Intercomparison Project (ISIMIP) produced under Coupled Model Intercomparison Project Phase 6 (CMIP6). IPSL-CM6A-LR represented the most recent version of the IPSL climate model. It provides oceanic forcing components such as chlorophyll, pH, temperature, dissolved oxygen concentration, sea water salinity, phytoplankton, and zooplankton, accessible at <https://data.isimip.org/>. It consisted of three models: for the atmosphere (LMDZ), for the land surface (ORCHIDEE), and for the oceans (NEMO). The ocean models included physics, sea-ice dynamics, and biogeochemistry (lower trophic level, carbon cycle with the main nutrients (P, N, Fe, and Si)) (Boucher et al., 2020).

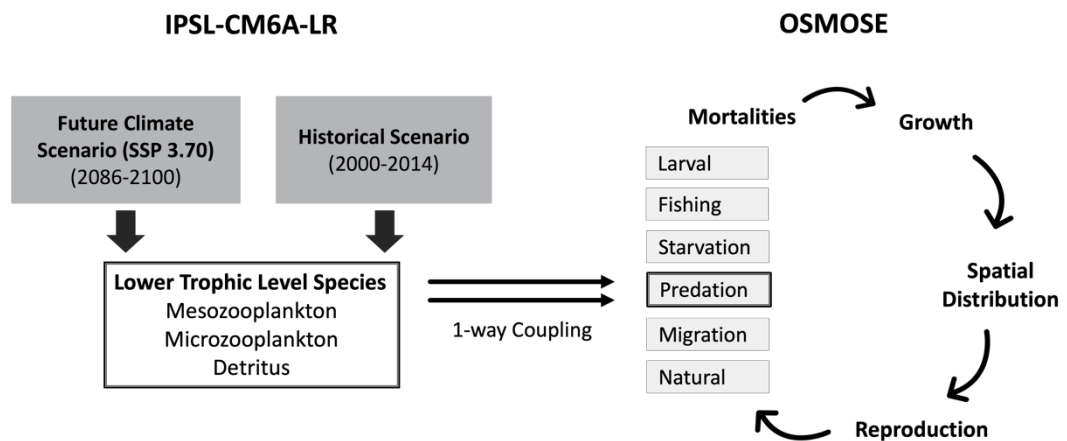


Figure 4. Conceptual representation of the OSMOSE-BS end-to-end model. The OSMOSE model was forced by the IPSL-CM6A-LR model through the predation of fish species on lower trophic levels.

### **2.2.1 Scenarios**

Two simulation scenarios were considered. The first scenario represented the historical period of the Black Sea from 2000 to 2014, and the second, the future climate change scenario, represented the impacts of climate change for the period 2086 to 2100. The future climate scenario was based on a future IPCC scenario (SSP 3.70), which was a combination of the Shared Socioeconomic Pathway 3 (SSP3) and the Representative Concentration Pathway 7.0 (RCP7.0) scenarios. It represented a medium to high future emissions and warming, particularly characterized by continuously high greenhouse gas emissions with a high radiation, i.e.,  $7 \text{ W/m}^2$  (van Vuuren et al., 2014).

### **2.2.2 Low Trophic Levels from IPSL-CM6A-LR**

The lower trophic level data, i.e., phytoplankton, mesozooplankton, and microzooplankton biomasses, were obtained for historical and future climate scenarios from the products of the low-resolution global climate model IPSL-CM6A-LR.

All lower trophic level data were global at a  $1^\circ \times 1^\circ$  spatial and monthly temporal resolution. To adapt these global data to the Black Sea for the OSMOSE model, they were remapped fit the geographic area of the Black Sea, which is between  $40.8^\circ \text{ N}$  to  $47^\circ \text{ N}$  in latitude and  $27.6^\circ \text{ E}$  to  $42.08^\circ \text{ E}$  in longitude. The inverse distance-weighted interpolation method was applied for all time steps using CDO (Climate Data Operators) to Black Sea grid, consisting of 22750 grid cells in total, (125 cells in the latitude, 182 cells in the longitude). This method performed a distance-weighted average of the four nearest neighbor values on all input data. Lastly, unit of all species was changed to tons and the monthly data was duplicated to two data for each month.

OSMOSE-BS model did not represent benthic invertebrates for the sake of simplicity; therefore, detritus was used as a resource to represent the portion of the

consumption that included invertebrates by benthic fish species. However, IPSL-CM6A-LR model products did not include detritus as a separate compartment; therefore, the biomass of detritus for the OSMOSE model was estimated using the formula proposed by Christensen and Pauly (1993) based on primary production and euphotic zone depth with the following equation:

$$\log D = 0.954 \log PP + 0.863 \log E - 2.41$$

where D = detrital biomass ( $gC/m^2$ ); PP=primary production ( $gCm^{-2}year^{-1}$ ); E = euphotic depth in 35 meter (Oguz et al., 1996).

The size ranges and trophic levels of plankton groups used in the HTL model were shown in Table 1. Fish species in the OSMOSE-BS model can access species at lower trophic levels based on predefined plankton accessibility rates considering environmental preferences and spatial overlap between species.

Table 1 Parametrization of the LTL

Low Trophic Level	Groups	Min Size (cm)	Max Size (cm)	Trophic Level
Mesozooplankton	Zo	0.02	2	2
Microzooplankton	Zm	0.002	0.02	2
Detritus	Dn	0.2	5	2.5

### 2.2.3 High Trophic Levels

OSMOSE represent its state variables by means of a school of individuals sharing the same characteristics of age, size, weight, diet, geographical location, and interactions with other schools. Between schools of species, growth and mortality rely on stochasticity, and interactions of schools were spatially defined by a size-based opportunistic predation model. (Shin & Cury, 2001, 2004). The key hypothesis between these schools was that opportunistic predation depends on the size

suitability and spatio-temporal co-occurrence between a predator and its prey. Thus, each individual can potentially feed on any prey depending on size availability, regardless of its taxonomy. Hence, maximum and minimum predator/prey size ratios were determined to control prey-predator interactions so that LTL organisms were not eaten exclusively by large predators. Also, in this two-dimensional horizontal spatial grid, a predator and its prey can encounter each other even if there is no overlap in their distribution in the water column as there OSMOSE model does not have an explicitly-resolved vertical spatial dimension (Shin & Cury, 2001, 2004; Travers et al., 2009; Travers-Trolet et al., 2014).

The change in a state variable over time was represented by

$$\frac{dS_i}{dt} = \frac{2\Delta L}{1 - \xi_{crit}} (\xi_i - \xi_{crit}) \times S_i - a_{j'} * B_{j',t} * \min\left(1, \frac{r * B_{i,t}}{\sum a_{j'} * B_{j',t}}\right) \times S_i \times S_j - (N_{i,t} * e^{-\Delta t * (M_{starv} + M_l + M_N + M_F + M_{out})}) \times S_i$$

where  $S_i$  is the modeled fish species,  $t$  is time,  $S_j$  is the predator species of  $S_i$ ,  $\Delta L$  is the mean growth rate in length,  $\xi_i$  and  $\xi_{crit}$  stand for the predation and the critical predation efficiencies,  $B_{i,t}$  is the biomass of a school  $i$  at time  $t$ ,  $j'$  indexes all local prey in the grid cell within the feeding size range of school  $i$ ,  $a_{j'}$  is the predation accessibility coefficient of the prey  $j'$  to  $i$ ,  $r$  the maximum predation rate,  $N$  is the abundance of a school,  $M_{starv}$ ,  $M_l$ ,  $M_N$ ,  $M_{out}$ ,  $M_F$  stand for starvation, larval, natural, migration and fishing mortality rates. The time step of the model set to two-week period.

#### a. Growth

Fish schools need a sufficient amount of food to grow in size and weight at a given time. For species to be able to grow, the predation efficiency  $\xi_i$  need to be greater than the critical value  $\xi_{crit}$ ; otherwise, starvation mortality occurs.

$$\Delta L_{(s,a,t)} = 0 \quad \text{if } \xi_i < \xi_{crit}$$



$$\Delta L_{(s,a,t)} = \frac{2\Delta L_{(s,a)}}{1 - \xi_{crit}} (\xi_i - \xi_{crit}) \quad \text{if } \xi_{crit} < \xi_i$$

$\Delta L_{(s,a,t)}$  is the increase in length of fish species  $s$  of age  $a$  during the time step  $t$ .  $\Delta L_{(s,a)}$  stands for the mean growth rate in length of fish species  $s$  of age  $a$  calculated from the von Bertalanffy model:

$$\Delta L_{(s,a)} = L_{\infty_s} (1 - e^{-K(a-t_0)})$$

$L_{\infty}$  stands for asymptotic length for species  $s$  of age  $a$ ,  $K$  is the growth coefficient ( $\frac{1}{\text{year}}$ ) and  $t_0$  is hypothetical age in years.

The body weight of species  $s$  at age  $a$  during the time step  $t$ ,  $W_{(s,a,t)}$ , is computed from length  $\Delta L_{(s,a,t)}$

$$W_{(s,a)} = c\Delta L_{(s,a,t)}^b$$

where  $c$  and  $b$  stand for two species-specific parameters, condition factor and allometric power coefficient, respectively.

## **b. Mortality**

Six different sources of mortality exist in the model, predation, starvation, larval, natural, and migration mortality, and were calculated at each time step in the model.

### **i. Predation Mortality:**

Predation is an opportunistic process depending on the prey-predator size ratio, and spatio-temporal co-occurrence between the predator and its potential prey (Shin & Cury, 2004). Considering the prey-predator size ratio, the predator can feed on any prey when its length provides the condition:

$$R_{min} \leq \frac{L_{pred}}{L_{prey}} \leq R_{max}$$

where  $R_{min}$  and  $R_{max}$  are the minimum and maximum predator/prey size ratios in length. The minimum and maximum lengths of a prey that a predator can eat are calculated as:

$$L_{max} = \frac{L_{pred}}{R_{max}}$$

$$L_{min} = \frac{L_{pred}}{R_{min}}$$

The degree of accessibility between species was defined through an accessibility coefficient matrix, which considers the difference in position within the water column of the predator and prey.

## ii. Starvation Mortality

Starvation mortality ( $M_{starv}$ ) affects fish groups when the food amount is too low to supply the primary body maintenance requirements for the species. This is observed when the predation efficiency ( $\xi_i$ ) is below the critical predation efficiency ( $\xi_{crit}$ ) ( $\xi_i < \xi_{crit}$ ).

The number of fish ( $N_{i,t}$ ) of species  $i$  at time  $t$  that starved is computed as:

$$N_{i,t+\Delta t} = N_{i,t} * e^{-\Delta t * M_{starv}}$$

with the starvation mortality rate which is:

$$M_{starv} = M_{max} \times \left(1 - \frac{\xi_i}{\xi_{crit}}\right) \text{ When } \xi_i < \xi_{crit}$$

where  $M_{max}$  is the maximum starvation mortality rate.

iii. Larval Mortality

Larval mortality ( $M_l$ ) represents the loss of eggs and first-feeding larvae from the model.

$$N_{i,t+\Delta t} = N_{i,t} * e^{-\Delta t * M_l}$$

iv. Natural Mortality

Natural mortality ( $M_N$ ) is a type of additional natural mortality that is not accounted for in the model explicitly. This additional mortality can be caused by factors such as diseases or predation by species not included in the model.

$$N_{i,t+\Delta t} = N_{i,t} * e^{-\Delta t * M_N}$$

v. Migration Mortality

Migration mortality ( $M_{out}$ ) is a way of accounting for deaths that occur outside of the model domain. It is used when species are not located within the simulation area for their entire life, and there could be a movement of biomass into or out of the domain.

$$N_{i,t+\Delta t} = N_{i,t} * e^{-\Delta t * M_{out}}$$

vi. Fishing Mortality

Fishing mortality ( $M_F$ ) depends on the annual fishing mortality rate  $M_F$  to the size of any fish schools larger than the recruitment size. The fishing mortality parameter was uniform over space. The survivors were calculated by:

$$N_{i,t+\Delta t} = N_{i,t} * e^{-\Delta t * M_F}$$

### c. Reproduction

When the length of the fish is greater than the length of first sexual maturity, the reproduction process takes place at the end of each time step if the species is in its defined reproduction season. The number of eggs depends on the relative fecundity  $\Phi_s$ , the sex ratio  $Ratio_{sex}$ , spawning biomass  $SB_{s,t}$  and reproduction seasonality.  $B_{s,i,t}$  is the total biomass of fish species  $s$  of fish group  $i$  at time  $t$  at the mature level.

$$N_{s,0,t+1} = \Phi_s * Ratio_{sex} * SB_{s,t} * Seasonality$$

$$SB_{s,t} = \frac{1}{2} \sum_{L_{s,i,t} \geq L_{MS}} B_{s,i,t}$$

### d. Spatial Distribution

The distribution of HTL species at the beginning of a simulation is random and prescribed based on spatial presence/absence or probability of occurrence maps. Additionally, species are confined to their respective distribution maps and cannot move to any adjacent cell outside their designated area (Shin et al., 2004). The model features two types of movements. First, the spatial distribution maps provide seasonal migrations for species per age and season. Second, when the population distribution map remains unchanged from one-time step to the next, schools randomly relocate to an adjacent cell (Travers-Trolet et al., 2014).

#### 2.2.3.1 Model parametrization of OSMOSE-BS

The OSMOSE-BS model was set up to represent eight commercially important fish species; three small pelagic fish species: European anchovy (*Engraulis encrasicolus*; Linnaeus, 1758), European sprat (*Sprattus sprattus*; Linnaeus, 1758), Mediterranean horse mackerel (*Trachurus mediterraneus*; Steindachner, 1868), and three demersal fish species: red mullet (*Mullus barbatus*; Linnaeus, 1758), whiting

(*Merlangius merlangus*; Linnaeus, 1758), turbot (*Scophthalmus maximus*; Linnaeus, 1758), and two pelagic piscivorous fish species: bluefish (*Pomatomus saltatrix*; Linnaeus, 1776), bonito (*Sarda sarda*; Bloch, 1973).

European anchovy spawn in the upper warm layer above the thermocline, at depths ranging from 0 to 25 meters. Its spawning occurs from mid-May, when water temperatures is 15-16°C, through to mid or late August, when temperatures rise to 25-26°C (Lisovenko & Andrianov, 1996). Sprat adults often stay below the thermocline and only go upwards during the spring and autumn. They spend the winter at depths of 80–100 meters, then close to the littoral area in April and May. During the summer, they avoid high water temperatures and migrate from the coast to the open sea. Mediterranean horse mackerel can be found in depths ranging from 5 to 250 meters. In spring, they migrate northward for reproduction and feeding. During the summer, they are distributed in the shelf waters above the thermocline (Ivanov & Beverton, 1985). Red mullet primarily inhabits sandy and muddy coastal areas and is distributed throughout the Black Sea region. Whiting can be found at depths of 10–120 meters throughout the coastal zone of the Black Sea. Their juveniles are pelagic and live above the 10-meter water layer, while adults prefer colder conditions where the temperature ranges from 6 to 10°C. Turbots are distributed across the entire coastal shelf. In spring, they spawn near the coast at depths of 20–50 meters, while in summer, they inhabit depths of 40–90 meters. During winter, they move to the open sea at depths of 50–140 meters. Bonito and bluefish migrate from the Sea of Marmara to the Black Sea for spawning during the warmest months and return back to the Sea of Marmara in the cold season.

The growth and reproduction parameters of the fish species were shown in

. The critical predation efficiency  $\xi_{crit}$  and the maximum ingestion rate was set to 0.57 and  $3.5 \text{ } gg^{-1} \text{ } year^{-1}$ , respectively (Gislason & Helgason, 1985; Laevastu & Larkins, 1981; Longhurst & Pauly, 1987). Reproduction seasons of eight HTL species were shown in Figure 5. All parameters were obtained from literature (Appendices A., Table A.1, and Table A.2 for reference list).

Table 2. Growth and reproduction parameters of OSMOSE-BS for eight HTL species.  $L_\infty$ ,  $K$ , and  $t_0$  are the von Bertalanffy growth parameters;  $c$  is Fulton's condition factor, and  $b$  is the exponent of the length-weight ( $L$ - $W$ ) allometric relationship.  $Ratio_{sex}$  is the ratio females to males in the population.  $\Phi_s$  is the relative fecundity,  $L_{mat}$  represents the length at first maturity.

	$L_\infty$	$K$	$t_0$	$c$	$b$	Seeding Biomass	$Ratio_{sex}$	$\Phi_s$	$L_{mat}$	Egg Size	Life Span
Anchovy	16.37	0.425	-1.35	0.005	3.043	624126.3	0.613	800	7	0.15	4
Sprat	13.76	0.42	-1.09	0.006	3.003	201474.9	0.577	277	7.8	0.1	5
Horse	20.5	0.231	-2.997	0.004	3.287	35692	0.436	287	12.2	0.0825	7
Mackerel											
Red	27.4	0.14	-2.351	0.009	3.033	17216.1	0.66	168.25	11.3	0.036	7
Mullet											
Whiting	37.9	0.16	-1.05	0.004	3.24	19331.1	0.57	246.87	14.5	0.11	9
Turbot	96.24	0.119	-1.01	0.011	3.139	6641.1	0.55	611	20.4	0.1149	11
Bluefish	51	0.228	-1.26	0.013	2.862	12000	0.59	305.4	25.4	0.105	3
Bonito	67.88	0.463	-1.22	0.01	3.085	22419	0.53	65	42.5	0.103	4

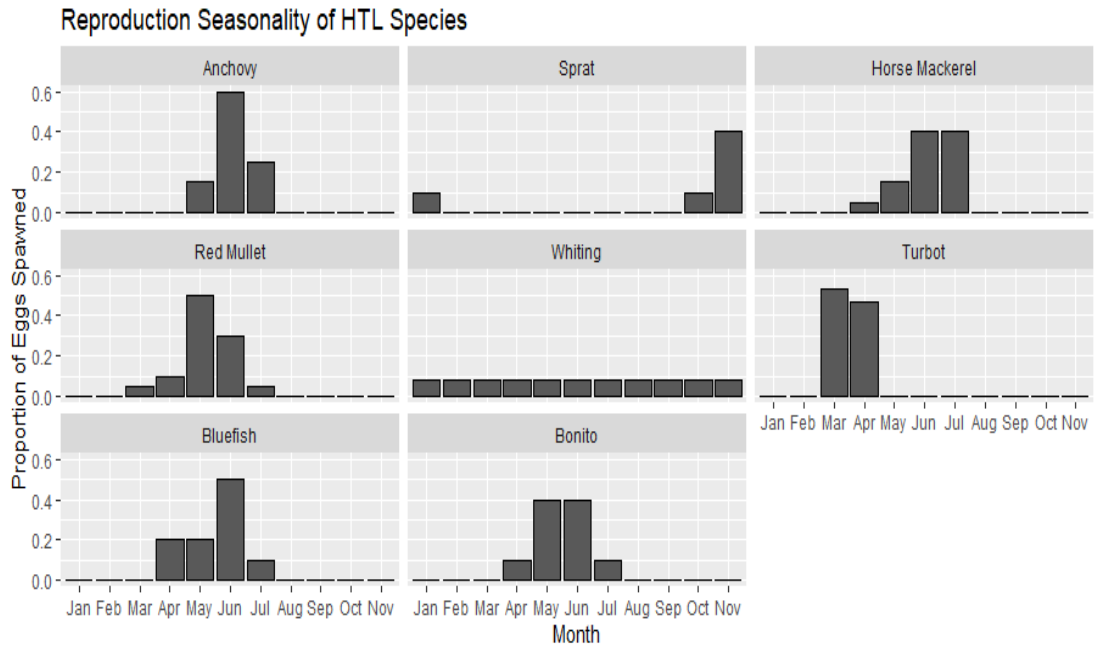


Figure 5. Reproduction seasonality for eight HTL groups.

The mortality parameters were given in Table 3. The maximum rate of starvation mortality  $M_{starv}$  was set to 0.3 for every species. The rate of larval mortality was set to 0.8 for every species. The migration periods of bluefish and bonito through the Istanbul Strait were in May and September, so they were present in the Black Sea during the summer months (Gordina, 1996; Zengin & Dinçer, 2006b). The mortality rates due to migration were considered during periods outside of these months for bluefish and bonito. An accessibility matrix defining proportional spatial overlap between predators and preys was defined based on spatial distributions of the species (Table 4).

Table 3. Mortality parameters of OSMOSE-BS for eight HTL species.  $M_F$ ,  $M_N$  and  $M_{out}$  are fishing, natural and migration mortality rates, respectively.  $R_{max}$  and  $R_{min}$  are maximum and minimum predator/prey size ratio.

	$M_F$	Recruitment Size	$M_N$	$M_{out}$	$L_{max}$	$R_{min}$	$R_{max}$
Anchovy	1.01	6	1		15	300	8
Sprat	0.91	9	0.73		13	300	8
Horse Mackerel	1.5	9	0.5		20	70	8
Red Mullet	0.98	6	0.69		21	13	6
Whiting	0.76	19	0.22		31	25	7
Turbot	0.5	18	0.22		82	18	7
Bluefish	0.98	18	0.44	0.98	36	14	7
Bonito	0.42	20	0.64	0.42	64	14	7

Table 4. Accessibility matrix for anchovy(sp0), sprat(sp1), Med. horse mackerel (sp2), red mullet(sp3), whiting (sp4), turbot (sp5), bluefish (sp6), and bonito (sp7).

	sp0	sp1	sp2	sp3	sp4	sp5	sp6	sp7
sp0	1	0.6	0.8	0.3	0.3	0.3	0.25	0.25
sp1	0.6	1	0.8	0.3	0.3	0.3	0.25	0.25
sp2	0.8	0.8	1	0.3	0.3	0.3	0.25	0.25
sp3	0.3	0.3	0.3	1	0.8	0.8	0.075	0.075
sp4	0.3	0.3	0.3	0.8	1	0.8	0.075	0.075
sp5	0.3	0.3	0.3	0.8	0.8	1	0.075	0.075
sp6	0.25	0.25	0.25	0.075	0.075	0.075	1	0.8
sp7	0.25	0.25	0.25	0.075	0.075	0.075	0.8	1
Mesozoo.	0.8	0.8	0.8	0.03	0.03	0.03	0.25	0.25
Microzoo.	0.5	0.5	0.5	0.01	0.01	0.01	0.1	0.1
Detritus	0	0	0	0.1	0.1	0.1	0	0



The spatial distributions of the eight HTL fish species were modeled in the Black Sea. The model included two types of movements: i) prescribed migrations when migratory species, anchovy, bluefish and bonito, carried out prescribed movements along their migratory routes during seasonal migrations, and ii) random walk movement to neighboring cells for all other species as well as anchovy, bonito and bluefish when they were out of the migration season (Figure 6). The age classes ( $< 1$ ) that did not carry out migrations of the migratory bonito and bluefish were always represented in the model domain, and adults (age  $\geq 1$ ) were not represented in the Black Sea during the period they spent in the Sea of Marmara (Table 5).

Table 5. Migration season and ages for anchovy, bluefish, and bonito

Migratory Species	Season	Age
Anchovy Migration (1)	May, Sep	0-4
Anchovy Migration (2)	Apr, Oct	0-4
Anchovy Wintering	Jan, Feb, Mar, Nov, Dec	0-4
Anchovy Spawning	June, July, Aug,	0-4
Bluefish Migration	May, Sep	1-3
Bluefish Spawning	June, July Aug	1-3
Bonito Migration	May, Sep	1-4
Bonito Spawning	June, July Aug	1-4

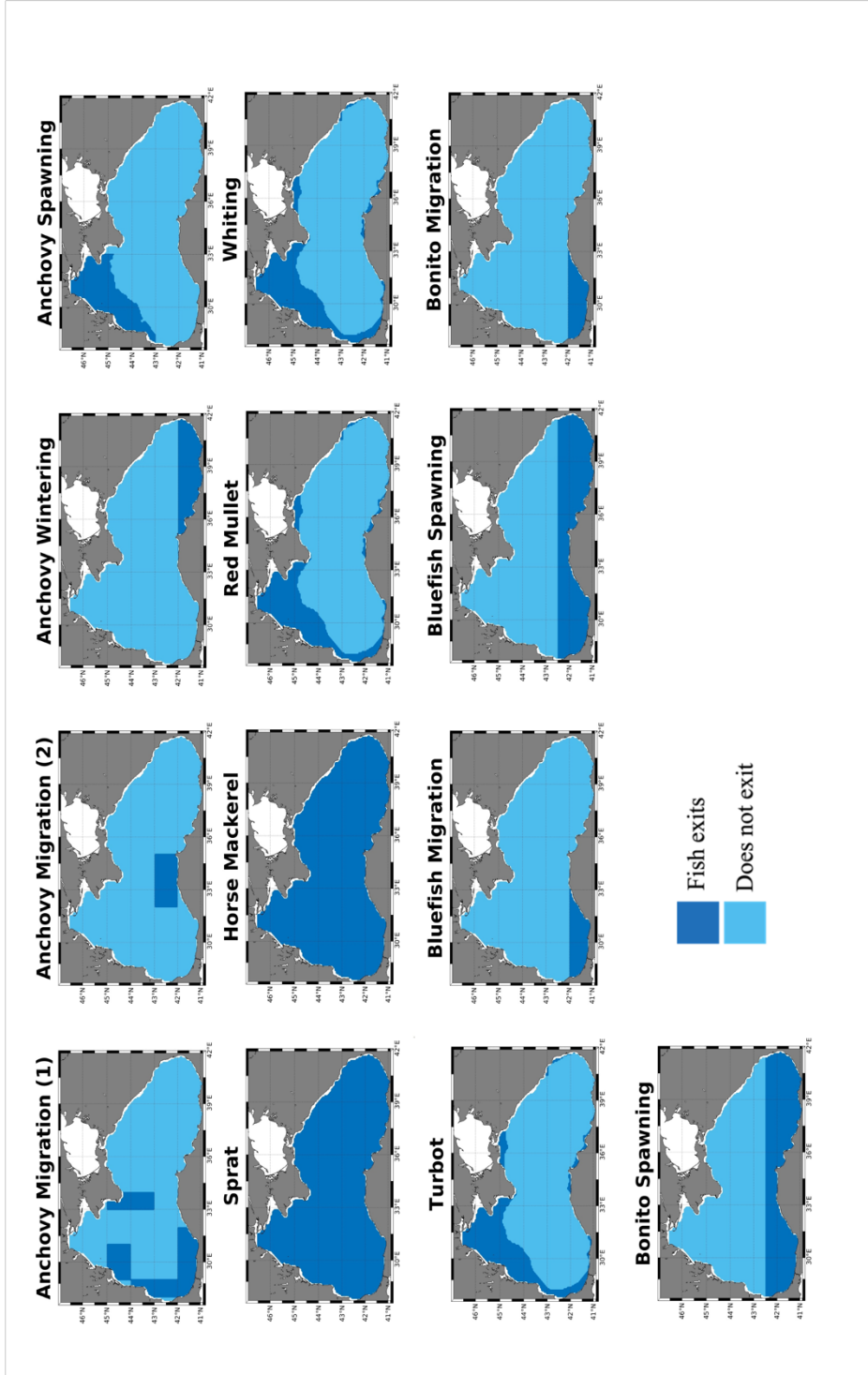


Figure 6. Prescribed spatial distributions, i.e., most likely occurrence, of HTL species in the OSMOSE-BS model.

### 2.3 Calibration of OSMOSE-BS

The calibration of OSMOSE-BS was accomplished by using an evolutionary algorithm (EA) to optimize the fit between the model and the time series of statistical catches and stock assessment predicted biomasses for the hindcast period. The EA was used to search for the best combination of model parameters that would produce the most accurate representation of the Black Sea marine ecosystem. This method, which involved using a likelihood approach specifically designed for the OSMOSE model, was implemented with the `osmose2R` and `calibrar` packages available on CRAN (the Comprehensive R Archive Network) (Oliveros-Ramos & Shin, 2016; Oliveros-Ramos et al., 2017 accessible at <https://cran.r-project.org/web/packages/calibrar/index.html>).

An evolutionary algorithm tests different combinations of unknown parameters to find the best solution, known as the "optimal parent," which is generated by combining the best-performing sets of parameters (genotypes). In each iteration of the optimization process (generation), many genotypes are tested, and the ones that perform the closest to the target data (simulated biomasses and landings) are used to create the optimal parent. This optimal parent is then used to make a new generation of parameter combinations through recombination or mutation. This process is repeated, with the optimal parent used to generate a new set of parameter combinations, until the algorithm reaches convergence of the objective function (Duboz et al., 2010; Oliveros-Ramos & Shin, 2016; Oliveros-Ramos et al., 2017).

OSMOSE-BS model was run for 100 years for each calibration, 86 years spin-up and 15 years of simulation, 28 replicates were used. The last 15 years were analyzed for the calibration. The unknown parameters were estimated in six different calibration phases. The phases included the following parameters with their maximum and minimum values: plankton accessibility for each plankton group, relative fecundity, the maximum ingestion rate, the additional mortality, the migration mortality rate for migratory species, and the fishing mortality rate for each HTL species (33 parameters

in total) (Appendices A. Table A.4). Phases of plankton accessibility for the plankton group and the migration mortality rate had 100 generations, while other phases had 300 due to computational constraints. To achieve more consistent results with the observed data, plankton accessibility for each plankton group, fishing mortality rate, maximum ingestion rate, and recruitment size were tuned manually after the calibration routine within the ranges in the literature.

Table 6. Recruitment sizes that were manually tuned after the calibration.

	Recruitment Size
Anchovy	6
Sprat	9
Horse Mackerel	9
Red Mullet	6
Whiting	19
Turbot	18
Bluefish	18
Bonito	20

## 2.4 Model Validation

To assess the model's consistency with observational data, biomass, catch, and mean size of catch results were compared in the hindcast scenario. Bluefish and bonito were not considered for biomass validation because of lack of data. To assess the skill of the model, the centered root mean square error was calculated between projections and observed data for biomasses and catches. The Spearman's rank correlation coefficient was used to compare simulated mean size at catch and observed data.

Observation data were shown in Appendices A, Table A.4 (for biomass), Table A.5 (for catch), and Table A.6 (for mean size of catch).

## **2.5 Analysis of the OSMOSE-BS's Results**

Ten simulation replicates were used considering OSMOSE-BS's stochasticity. The model projections were generated through the mean of ten replications and represented as a time series spanning 15 years, encompassing maximum and minimum intervals of replications.

The Mann-Whitney U test was applied for mesozooplankton, microzooplankton and detritus to assess significant changes between hindcast and forecast scenarios.

The changes in biomass, catch, and size values between future climate (2086-2100) and historical (2000-2014) scenarios were calculated by the fractional change, subtracting the historical projections from the future ones, and dividing by the projections of the historical period.



## **CHAPTER 3**

### **RESULTS**

In this chapter, the projections for the low trophic levels from the earth system model and the outcomes of the calibration of the OSMOSE-BS model were presented. To assess the model skill, the comparisons of model simulations and observation data of HTL species were demonstrated for the Black Sea, depending on their biomass, catch, and size. Thereafter, the model results for the forecast scenario were shown based on biomass, catch, and size at catch. Lastly, the forecast scenario was compared to the hindcast scenario for LTL and HTL species.

#### **3.1 Current and Future IPSL-CM6A-LR Projections**

Annually-averaged sea surface temperature changes in both scenarios were shown in Figure 7. IPSL-CM6A-LR projections for the Black Sea showed an increase in sea surface temperature in the future scenario.

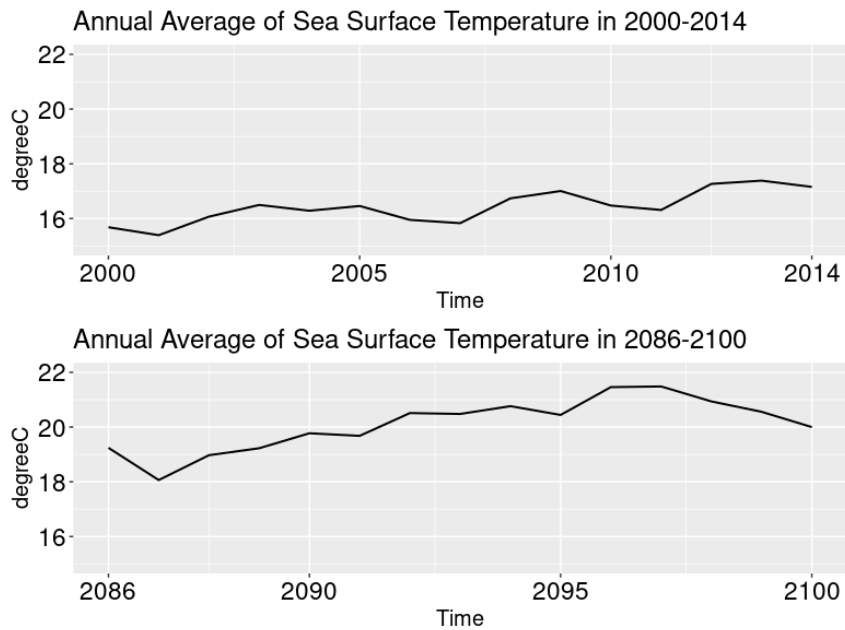


Figure 7. Annually-averaged time series of sea surface temperature for hindcast and forecast scenarios.

Projections of IPSL-CM6A-LR based on annual average biomass changes over time for mesozooplankton, microzooplankton and detritus were shown in Figure 8. The comparison between the forecast (2086-2100) and hindcast (2000-2014) scenarios revealed that the forecast scenario projected increases in biomass levels for all lower trophic level groups.

The annually-averaged vertically-integrated primary production, which was used to calculate the detritus group's biomass empirically, was calculated to increase in the forecast scenario (2086-2100) compared to the hindcast (2000-2014) scenario in the Black Sea (Figure 9).



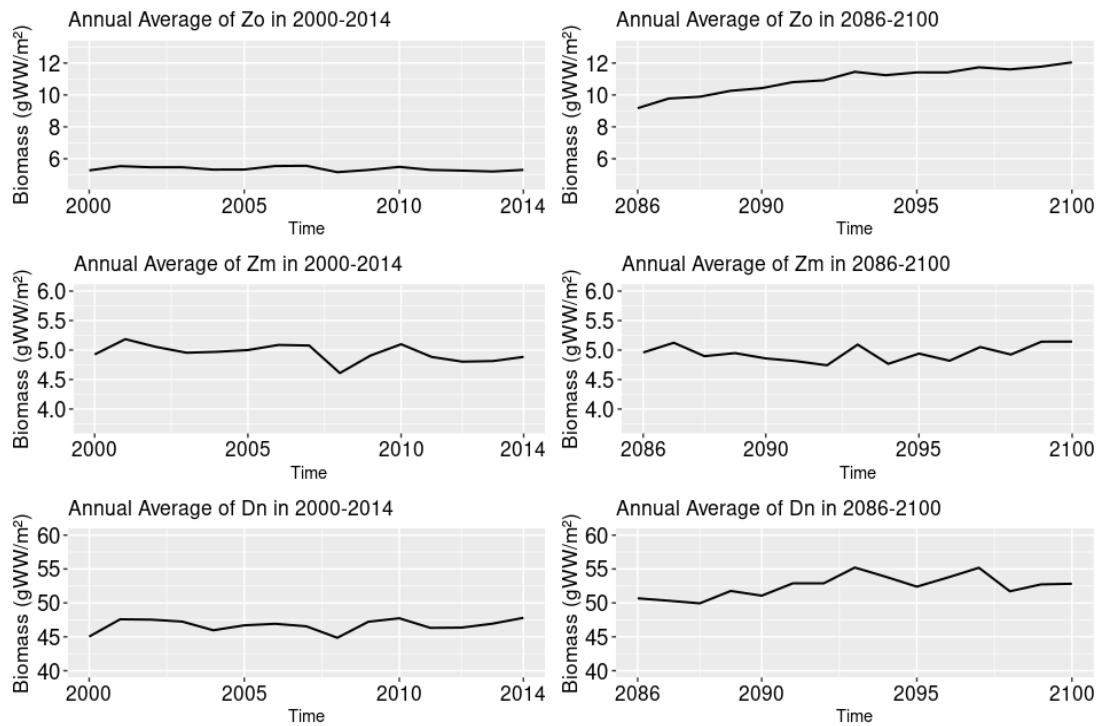


Figure 8. Annually-averaged time series of biomass of mesozooplankton (Zo), microzooplankton (Zm), detritus (Dn) in hindcast (left) and forecast (right) scenarios.

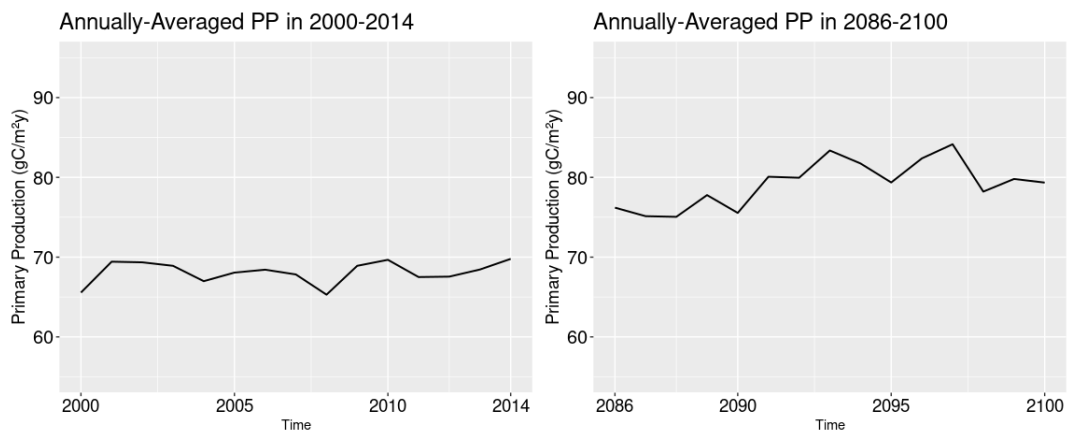


Figure 9. Annually-averaged time series of vertically-integrated primary production in hindcast (left) and forecast (right) scenarios.

### 3.2 Hindcast Simulation, Model Validation and Skill

Evolutionary algorithm used for the calibration does not necessarily reach convergence for the parameters based on the cost function; therefore, after automated calibration, adjustments were made to parameters such as plankton accessibility for each plankton group, fishing mortality rate, maximum ingestion rate, and recruitment size parameters to achieve better alignment with the observational data.

Six parameters (i) plankton accessibility for each plankton group, (ii) relative fecundity, (iii) the maximum ingestion rate, (iv) the additional mortality rate, (v) the migration mortality rate for migratory species, and (vi) the fishing mortality rate were estimated for the Black Sea (Table 7).

Table 7. Calibration parameters of OSMOSE-BS.

	Plankton Accessibility	Relative Fecundity	Max Ingestion Rate	$M_N$	$M_{out}$	$M_F$
Anchovy		662	1.12	1.07		2.89
Sprat		46	2	0.99		2
Horse Mackerel		66.2	10	1.12		0.6
Red Mullet		2860	10	0.928		2.7
Whiting		2310	10	0.635		0.6
Turbot		446	25	0.981		0.8
Bluefish		452	7.41	0.786	0.664	2.2
Bonito		42.1	7.49	0.651	0.614	1.87
Zo	0.45					
Zm	0.5					
Dn	0.07					

To assess the model's consistency with observational data, biomass, catch, and mean size of catch results were compared in the hindcast scenario. Simulated biomass

levels in the hindcast scenario over fifteen years (2000-2014) were presented in Figure 10 in comparison to stock assessment estimated biomasses (Appendices, Table A.4). Bluefish and bonito were excluded due to the absence of stock assessment studies for their stocks. For anchovy, sprat, horse mackerel, and turbot, the model generally overestimated their biomasses in most of the years. For red mullet, although the model closely matched the data between 2000 and 2003, it generally underestimated in subsequent years. However, the model results generally aligned well with the observed data.

Figure 11 showed the simulated catches in comparison to statistical catch data for the years 2000 to 2014 (Appendices, Table A.5). Generally, the simulated catch closely matched the statistical catches for all species. After 2002, the simulated whiting catch slightly overestimated the actual catches.

The centered root mean square error (cRMSE) values for all species based on biomass and catch were shown in Table 8. The lowest cRMSE for biomass was observed in horse mackerel at 0.96, while the highest was 1.04 for whiting. On the other hand, in terms of catch data, the highest cRMSE was 1.07 for anchovy, while the lowest was 0.96 for horse mackerel.

Table 8. The centered root mean square error.

Species	Biomass	Catch
Anchovy	1.005	1.07
Sprat	1.002	0.996
Horse Mackerel	0.96	0.96
Red Mullet	1.01	1.03
Whiting	1.04	1.01
Turbot	1.001	1.01
Bluefish	-	1.01
Bonito	-	0.97

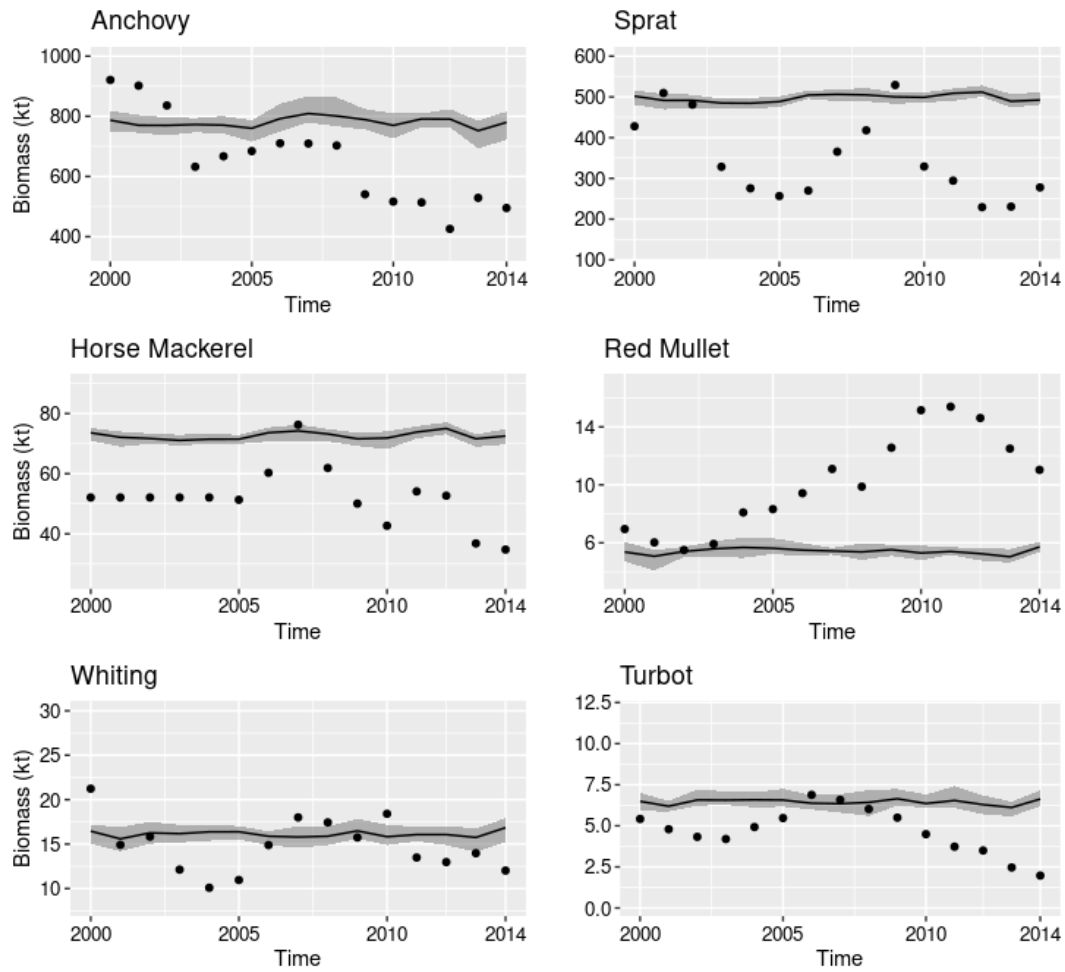


Figure 10. The comparison of simulated biomasses of six HTL species against stock assessment estimated biomasses over a 15-year hindcast simulation. The gray-shaded bands represent the maximum and minimum intervals obtained from 10 simulation replicates. The dots represent the stock assessment estimated biomasses.

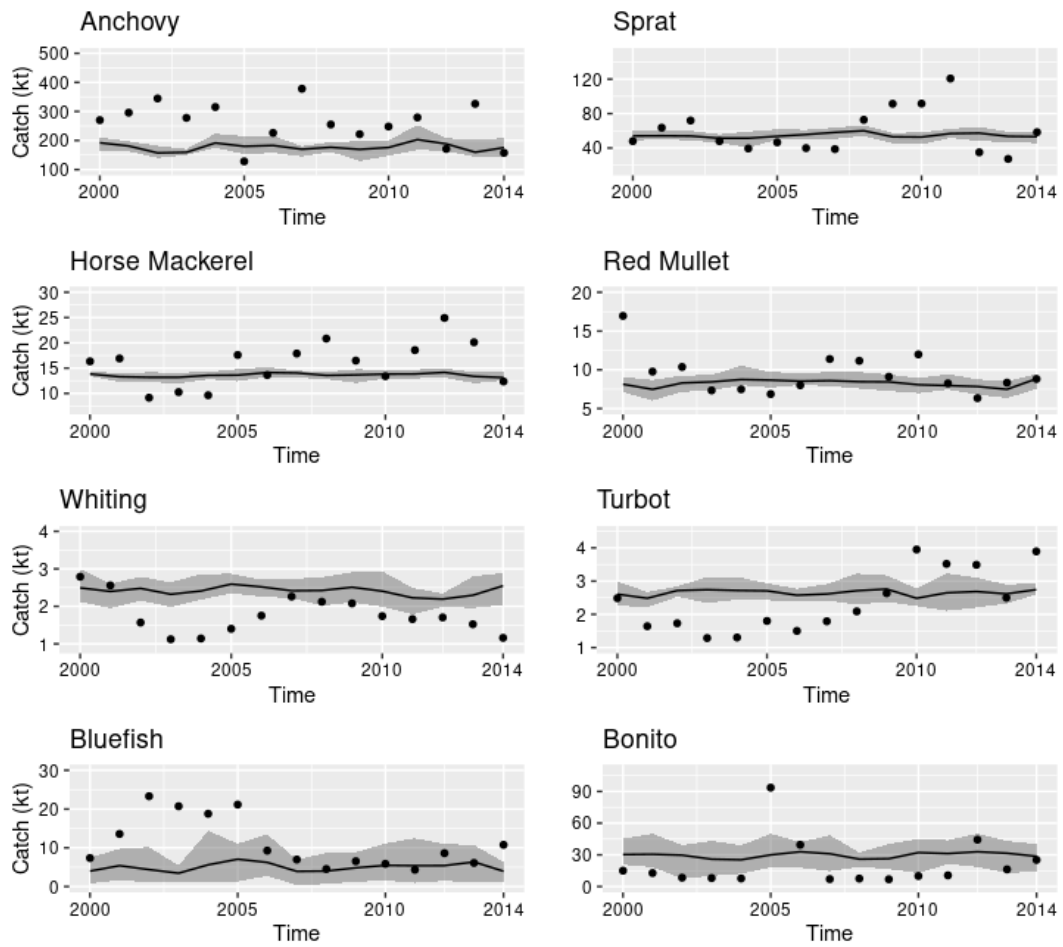


Figure 11. The comparison of simulated catches of eight HTL species against statistical catch data over a 15-year hindcast simulation. The gray-shaded bands represent the maximum and minimum intervals obtained from 10 simulation replicates. The dots represent the statistical catches.

Model simulated mean catch sizes for fish species were compared against literature data (Appendices, Table A.6) from the Black Sea (Figure 12). The mean catch sizes of anchovy, horse mackerel, and red mullet were slightly below their observed values. Conversely, the size of sprat was marginally above its observed value. The sizes for turbot and bonito were considerably lower than their observed sizes, whereas the size of whiting was notably higher than its reference point. The mean

catch size of bluefish aligned precisely with its observed value. The Spearman’s rank correlation coefficient between the simulated mean catch sizes and observed values was 0.74 (p-value = 0.0458).

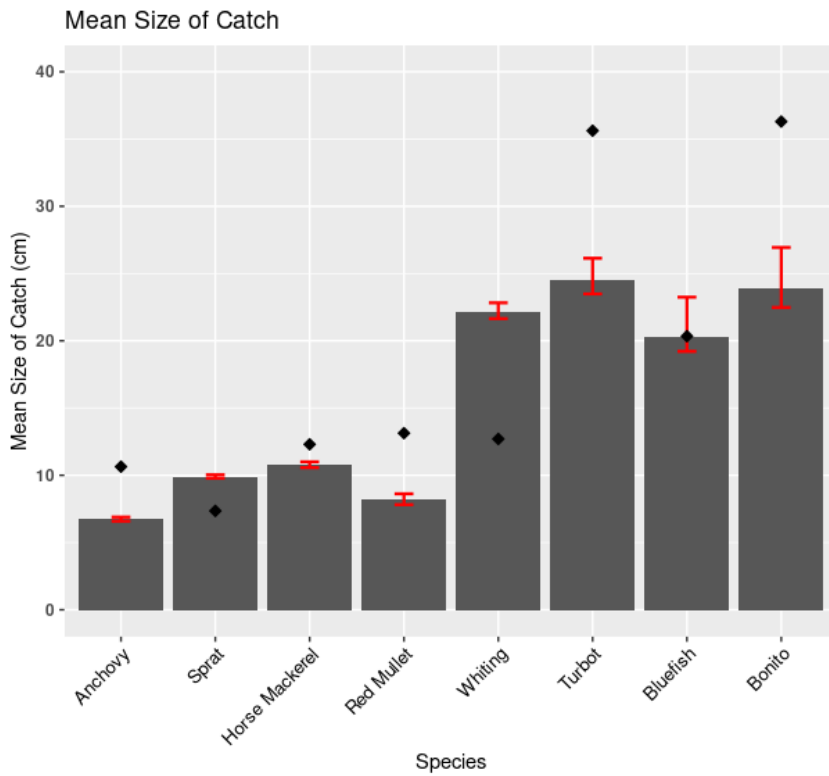


Figure 12. The mean size at catch for eight HTL species over the 15-year hindcast simulation. The vertical red bars correspond to the standard deviation of the simulations across 10 replicates. The black diamonds represent the observed sizes.

### 3.3 Forecast Simulation

The model results for the SSP 370 scenario, forecasting climate change impacts from 2086 to 2100, were presented in Figure 13 for biomass, Figure 14 for catch, and Figure 15 for mean size at catch level.

Figure 13 displayed the projected changes in mean biomass with the maximum and minimum ranges between 2086-2100 under the forecast scenario using the OSMOSE-BS model. In 2090, the small pelagic fish groups, including anchovy, sprat, and horse mackerel, reached their peak biomass values at 1348.3, 999.9, and 160.4 kilotons, respectively. However, a drastic decline was simulated soon after. The biomasses of anchovy and sprat were projected to reach their minima in 2093 at 1149.6 and 896.4 kilotons, respectively, while horse mackerel biomass reached its minimum value in 2092 at 134.9 kilotons. On the other hand, the biomasses of the demersal fish group, red mullet, whiting, and turbot, was projected to peak in 2087 at 7.1, 16.7, and 7.8 kilotons. By 2093, whiting and turbot biomasses had declined to their lowest biomass levels, at 17.1 and 6.7 kilotons, respectively. In contrast, the biomass of red mullet reached its minimum value of 5.8 kilotons in 2095. Bluefish achieved its maximum biomass of 244.1 kilotons in 2090, matching the highest values of the large pelagic fishes. Meanwhile, bonito peaked at 143.8 kilotons in 2087, coinciding with the year the biomasses of demersal fish reached their maxima. The lowest biomass levels projected for bluefish and bonito were 187.3 kilotons in 2092 and 106 kilotons in 2098, respectively.

The predicted variations in the mean catch values were shown in Figure 14. After 2090, the catches of the small pelagic fish group, anchovy, sprat, and horse mackerel, decreased to 246.8, 89.8, and 24.4 kilotons, respectively. Before this period, they reached their peak catch levels of 392.3, 132.3, and 30.8 kilotons, respectively. In 2087, the catches of red mullet and turbot peaked and simulated as 11.1 and 3.2 kilotons, respectively. By the end of the century, whiting was projected to reach its maximum catches of 3.1 kilotons. Bluefish's catch peaked at 14.3 kilotons in 2087 and reached its lowest value at 6.7 kilotons by 2093. However, bonito was expected to reach its highest catch of 75.8 kilotons in 2088 and the lowest at 51.4 kilotons in 2093.

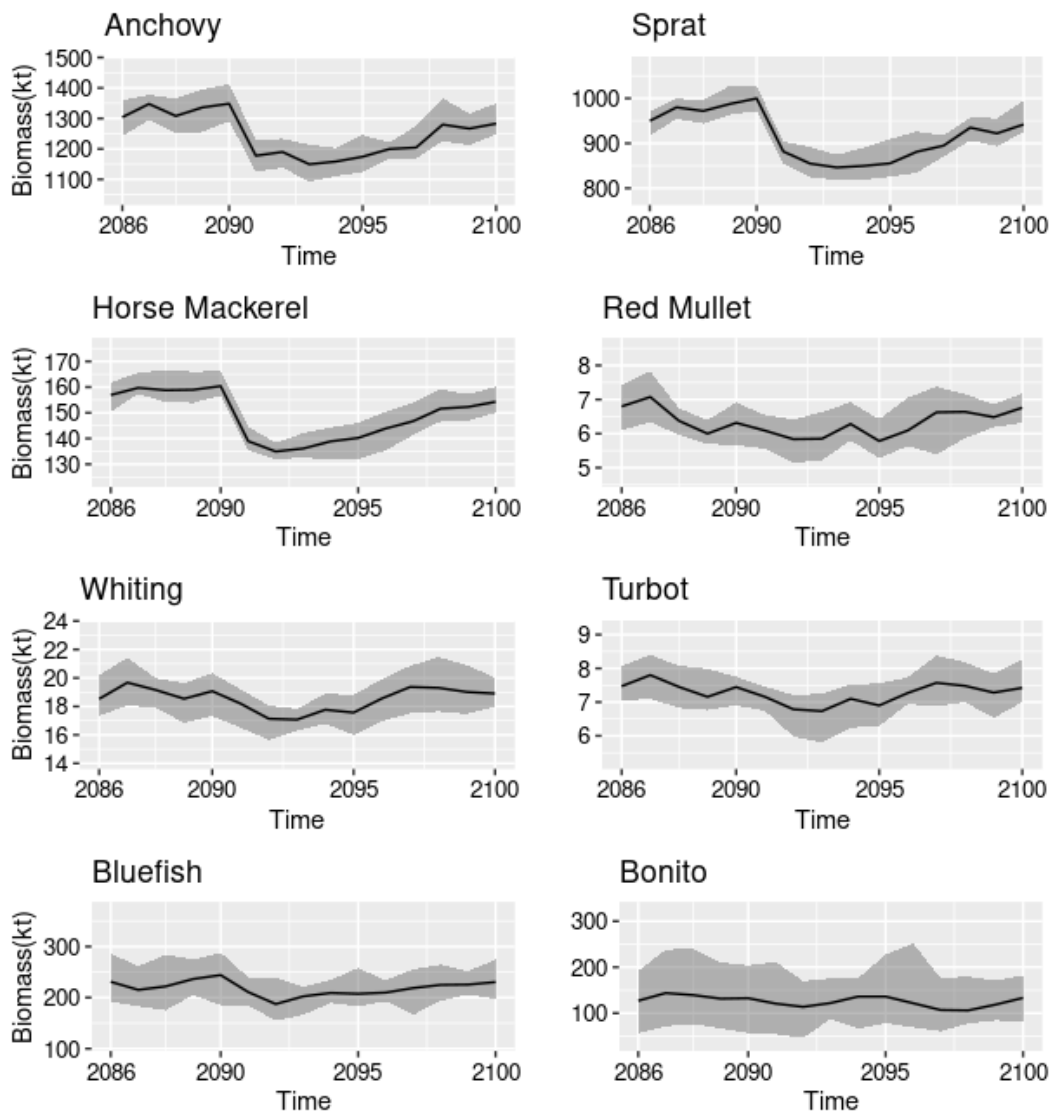


Figure 13. The mean biomass values predicted by OSMOSE-BS for the eight fish species during 2086-2100. The gray-shaded area represents the maximum and minimum intervals obtained from 10 simulation replicates.



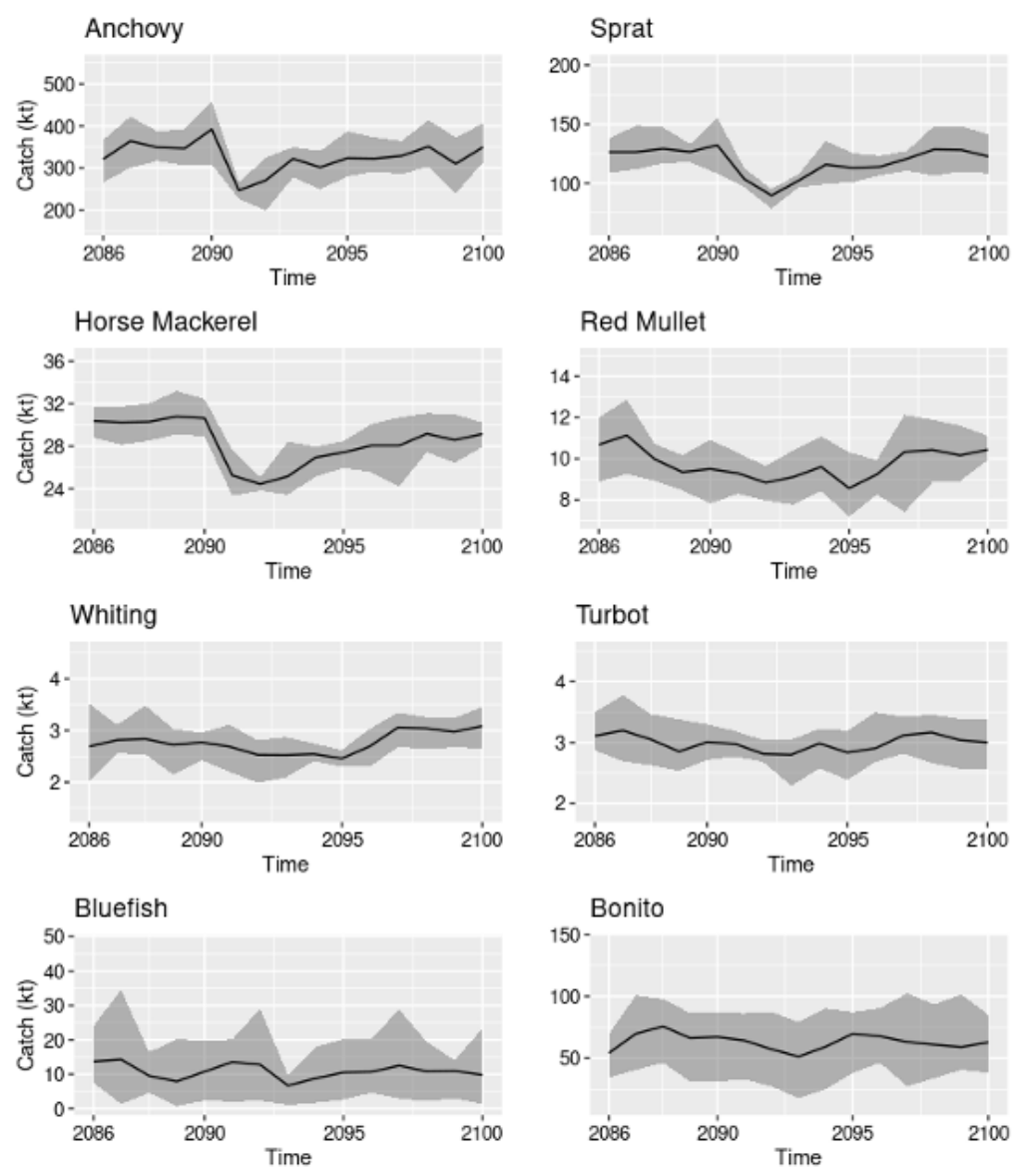


Figure 14. The mean catch values predicted by OSMOSE-BS of the eight fish species during 2086-2100. The gray-shaded area represents the maximum and minimum intervals obtained from 10 simulation replicates.

The mean catch sizes in the forecast scenario were 6.76 cm for anchovy, 9.89 cm for sprat, and 10.77 cm for horse mackerel (Figure 15). Considering demersal fish species, the sizes were 8.23 cm for red mullet, 22.16 cm for whiting, and 24.64 cm

for turbot. Additionally, bluefish and bonito had mean catch sizes of 20.13 cm and 23.82 cm, respectively.

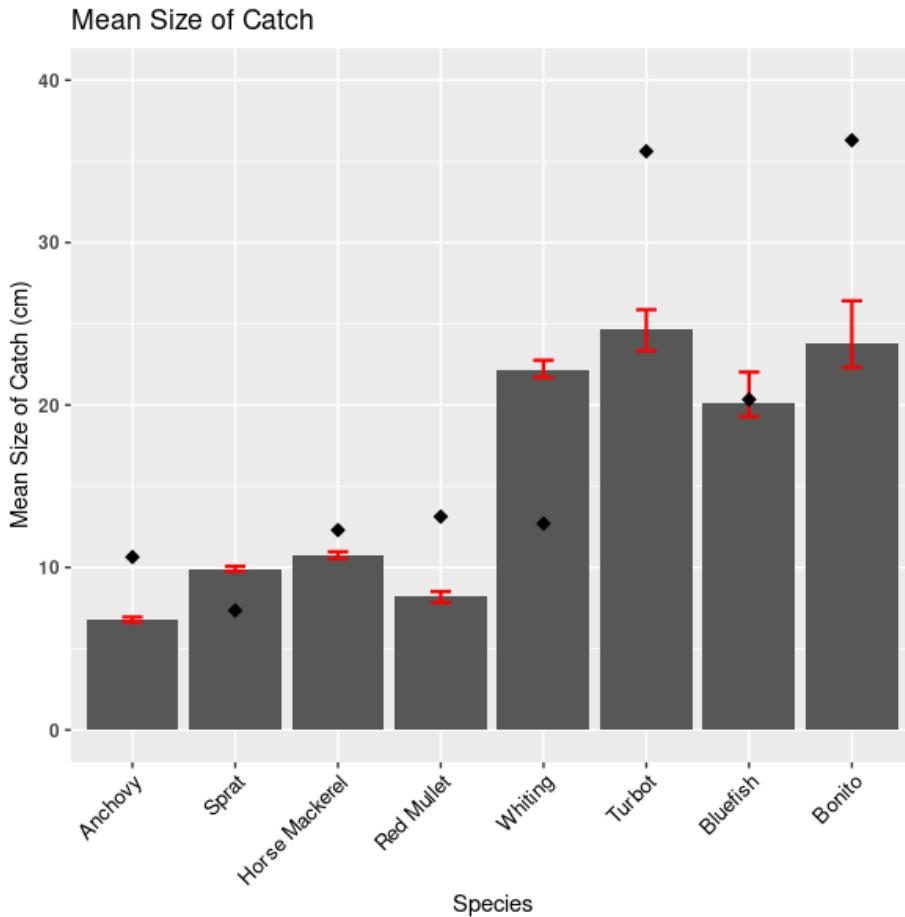


Figure 15. The mean size at catch in forecast scenario for the eight fish species during 2086-2100. The vertical red bars correspond to the standard deviation of the simulation across 10 simulation replicates. The black diamonds represent the observed sizes.

### 3.3.1 The Comparison Between Forecast and Hindcast Scenarios

Toward the end of the century, increases were observed in the biomass of all lower trophic level species, as shown in Figure 16. Mesozooplankton experienced a

significant increase according to the Mann–Whitney U test ( $p < 0.0001$ ), with a fractional change of 1.04. In contrast, microzooplankton did not exhibit a significant increase according to the Mann–Whitney U test ( $p = 0.78$ ), showing only a marginal rise of 0.0003. Detritus was simulated to increase significantly according to Mann–Whitney U ( $p < 0.0001$ ), corresponding to a fractional change of 0.124.

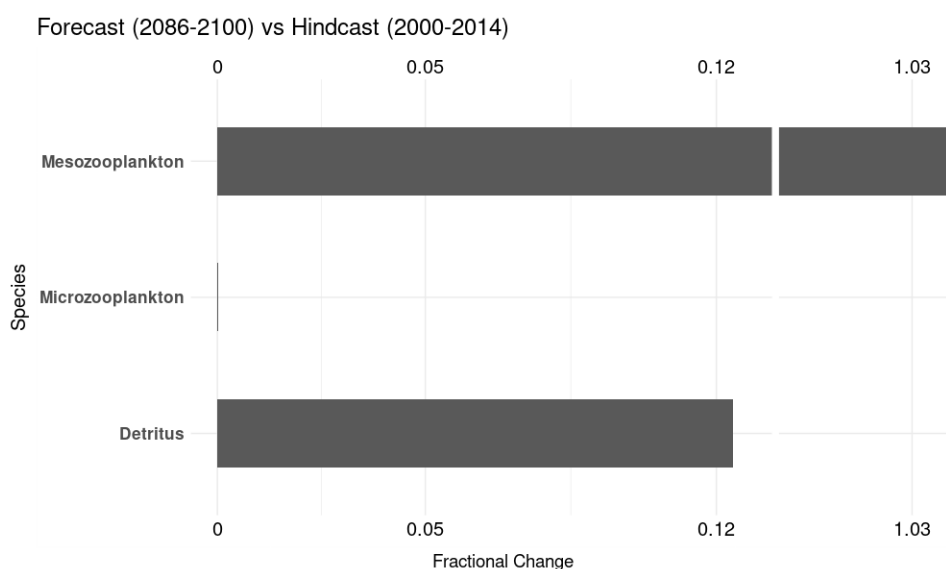


Figure 16. Fractional change in biomass of LTL species between forecast and hindcast scenarios.

Comparison of Forecast (2081-2099) and Hindcast (2001-2019) scenarios based on changes in the biomass and catch levels were shown in Figure 17. The findings revealed an increase in both biomass and catch for all species in the forecasted period (2086-2100) when compared to the hindcast period (2000-2014).

For changes in biomass, bonito showed an increase, with a positive fractional change of 1.34. Bluefish followed closely with an increase of 1.04. The demersal fishes, consisting of red mullet, whiting, and turbot, exhibited relatively lower increases with fractional changes of 0.17, 0.15, and 0.13, respectively. For the small pelagic

fish group, the fractional change was 0.6 for anchovy, 0.85 for sprat, and 1.05 for horse mackerel.

Until the end of this century, catch changes showed the highest increase in the large pelagic species, bluefish, with a fractional change of 1.2, followed closely by bonito at 1.16. This increase was followed by sprat with a fractional change of 1.18, and other small pelagic fish species as anchovy had an increase of 0.85 and horse mackerel had an increase of 1.08. Similar to the changes in biomass, demersal fishes had shown relatively lower increases. There had been a fractional change of 0.19 in red mullet, 0.15 in whiting, and 0.13 in turbot.

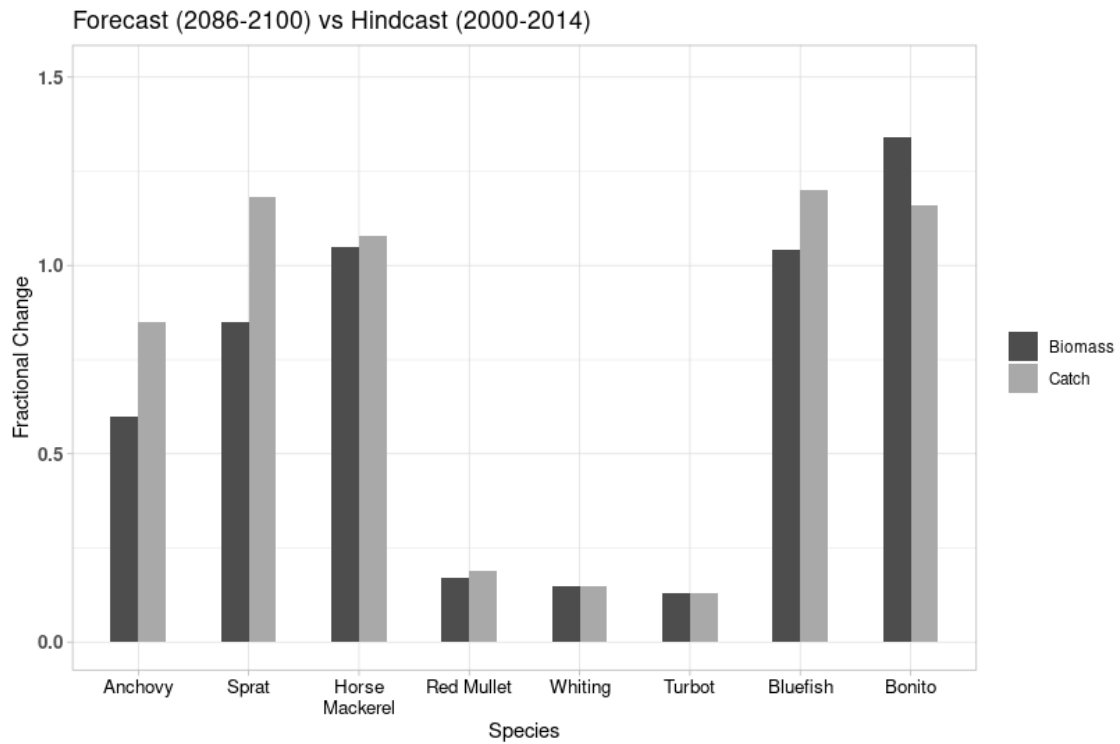


Figure 17. Fractional change in biomass and catch between forecast and hindcast scenarios.

The mean sizes of catch for anchovy, sprat, and turbot increased with fractional changes of 0.005, 0.0009, and 0.004, respectively. In contrast, the mean sizes of catch for horse mackerel, red mullet, whiting, bluefish, and bonito were projected to decline in the forecast scenario, with fractional changes of -0.001, 0.0002, 0.0008, 0.008, and 0.005, respectively (Figure 18).

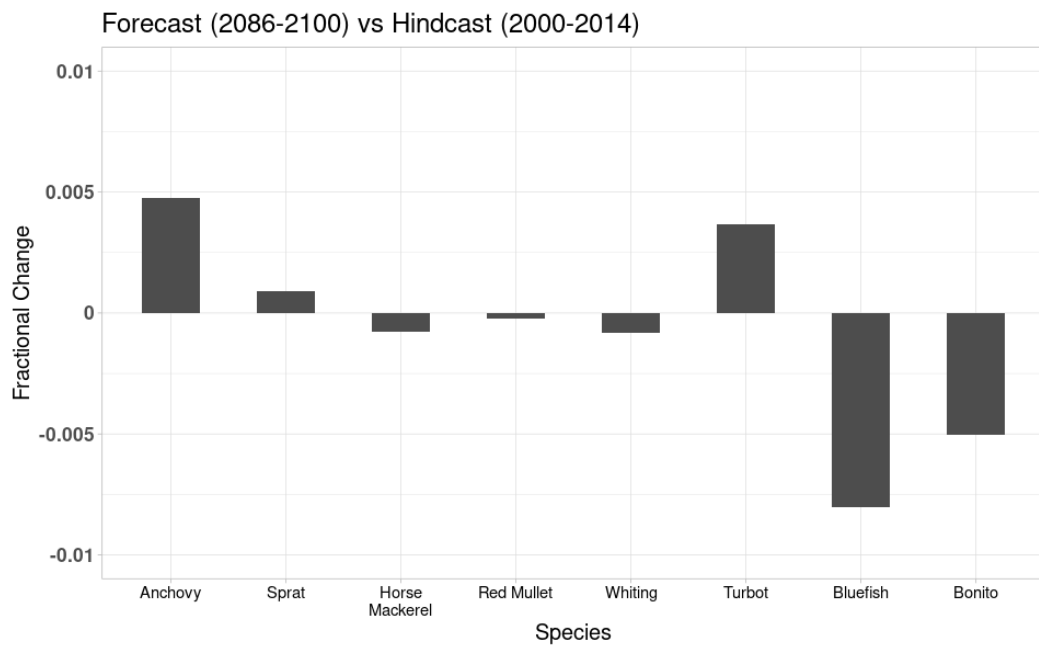


Figure 18. Fractional change in mean size of catch between forecast and hindcast scenarios.

The biomass distributions by size for small pelagic fish groups was projected to increase for all species across all size classes in the future (Figure 19). Specifically, for anchovies, the 1-2 cm size class exhibited the highest fractional change, with a value of 8.06. For sprat and horse mackerel, the highest increase was observed in the 2-3 cm size class, with a fractional change of 3.9 and 3.7, respectively.

The biomass distribution by size for the demersal species, red mullet, whiting, and turbot, indicated a relatively lower increase of biomass in all size classes compared to pelagic species, with a fractional change between 0.1 and 0.3 (Figure 20).

Considering large pelagic fish species, the biomass of bluefish had an increase in all size classes (Figure 21). Further, the biomass distribution in the future scenario for the 39–40 cm and 40–41 cm size classes of bluefish showed a substantial increase, with fractional changes of 721.7 and 409.9, respectively. Additionally, an increase of 0.002 tons was observed in the 41–42 cm size class in the forecast scenario. For bonito, the highest increase in biomass was obtained in the 6–8 cm size classes, with a fractional change of 16. Compared to the other species, a decrease in biomass was observed in the 67–68 cm size class, with a fractional change of 0.1. Moreover, bonito was expected to have a biomass of 0.01 tons in the 70–71 and 71–72 cm size ranges in the future scenario, that was not shown in the fractional change in Figure 21.

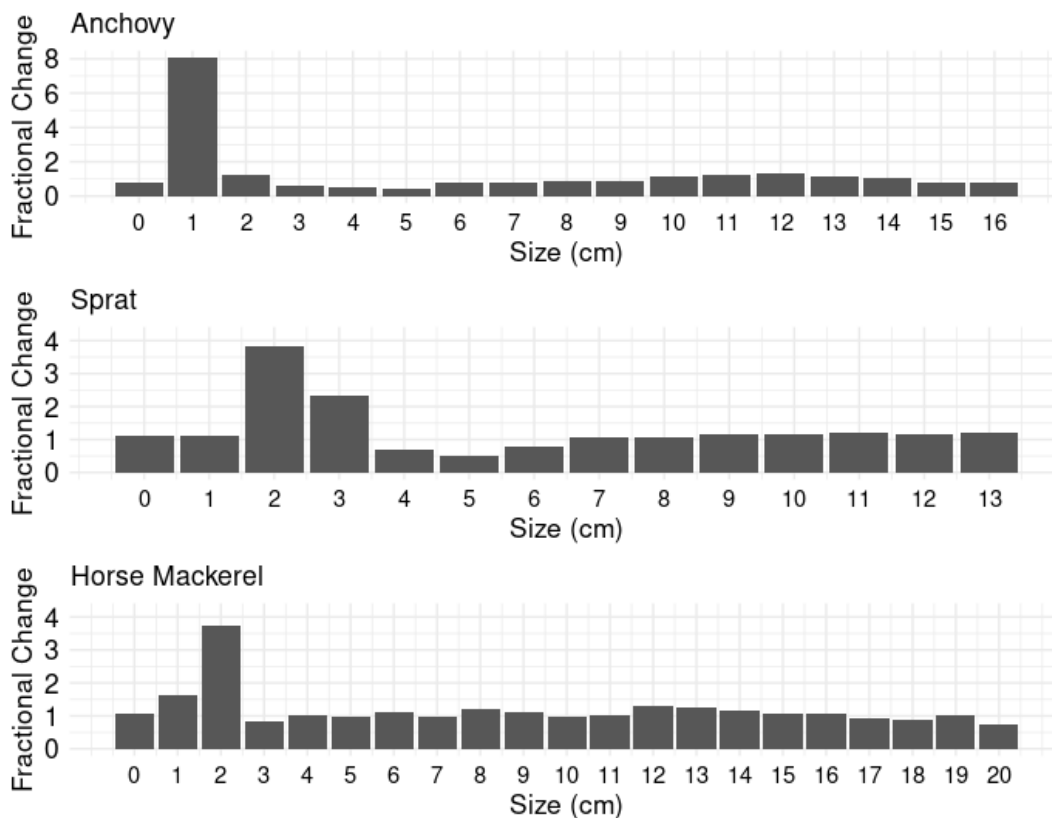


Figure 19. Fractional change of biomass distribution by size between forecast and hindcast scenarios for the small pelagic species' populations.

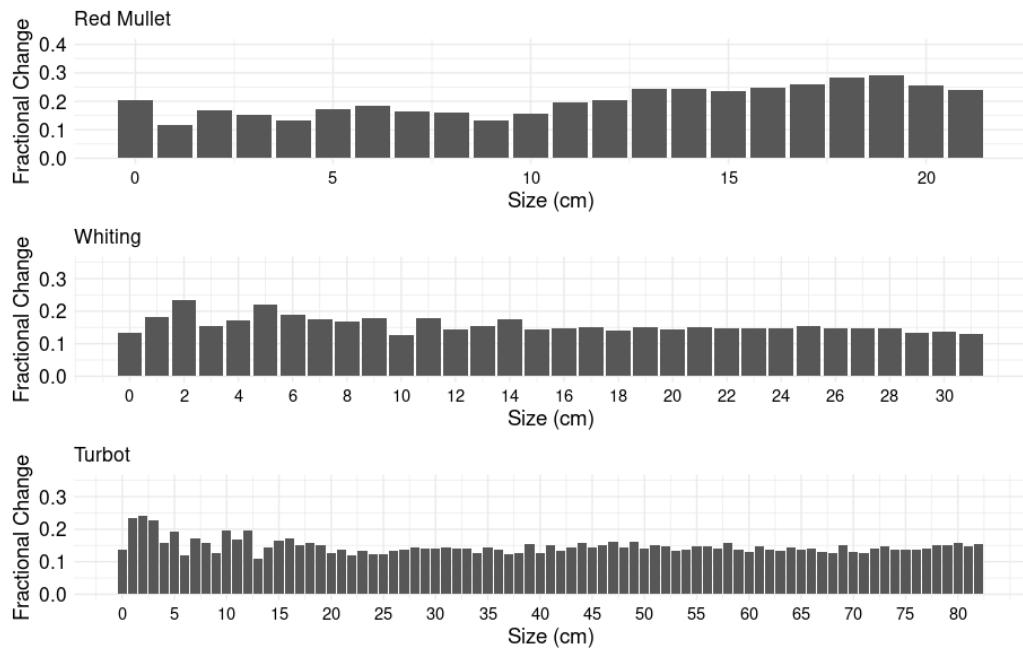


Figure 20. Fractional change of biomass distribution by size between forecast and hindcast scenarios for the demersal pelagic species' populations.

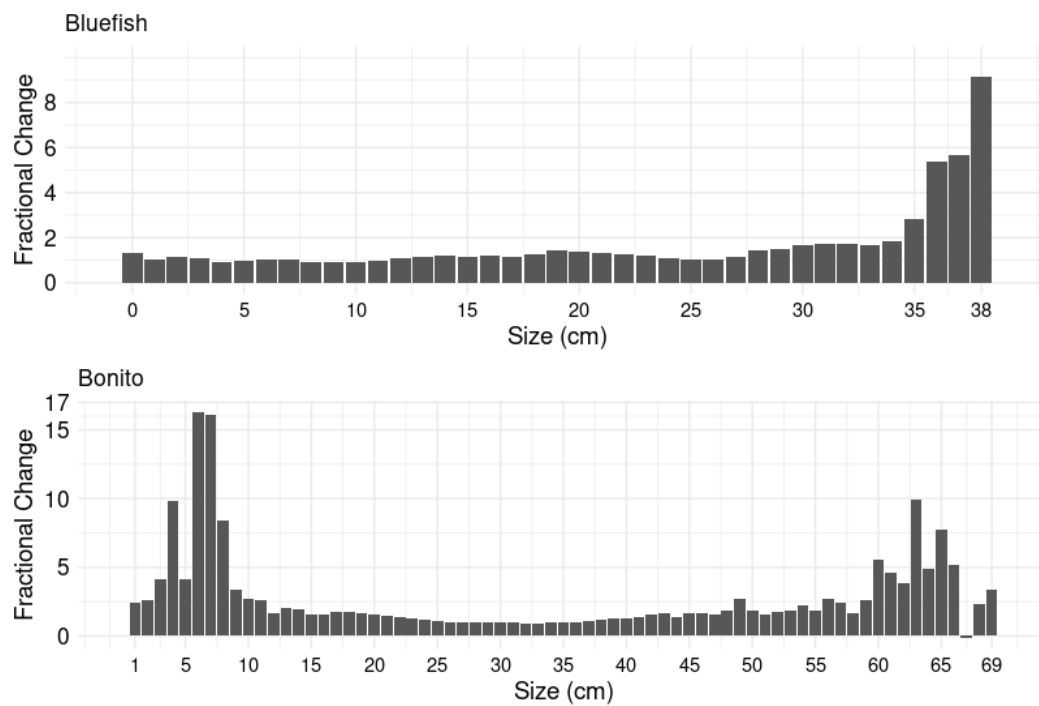


Figure 21. Fractional change of biomass distribution by size between forecast and hindcast scenarios for the large pelagic species' populations.

The proportion of species biomass across the minimum landing size was shown in Figure 22 for the small pelagic species, Figure 23 for the demersal species, and Figure 24 for the large pelagic species.

The proportion of anchovy biomass in the future scenario for 0–9 cm revealed a slight decrease of 0.3%, while the larger size class (>9 cm) was projected to increase by 26.7%. The proportion of sprat biomass for 0–9 cm decreased by 1.01%; however, the proportional biomass of the larger class (>9 cm) of sprat increased by 17.25%. No substantial difference was observed in the proportions of horse mackerel biomass for the 0–13 cm size class, whereas an increase of 0.98% was obtained for the larger size class of horse mackerel (Figure 22).

Figure 23 indicated a decrease of 1.18% in the proportion of red mullet biomass for the 0–13 cm size class, while the larger size class (>13cm) was projected to increase by 6.67%. The proportion of whiting biomass for the 0–3 cm size class increased by 0.81%, whereas the larger class (>13 cm) decreased by 0.59%. No substantial difference was obtained in the proportion of turbot biomass for the 0–45 cm size class; however, a decrease of 0.25% was observed for the larger class of turbot.

The proportion of bluefish biomass in the future scenario had a decrease of 0.27% for the 0–20 cm size class, while an increase of 12.39% was obtained for the larger size class (>20 cm). An increase of 5.88% was observed in the proportion of bonito biomass for the 0–25 cm size class. On the other hand, the larger class (>25 cm) of bonito showed a decrease of 18.6% in the future scenario (Figure 24).



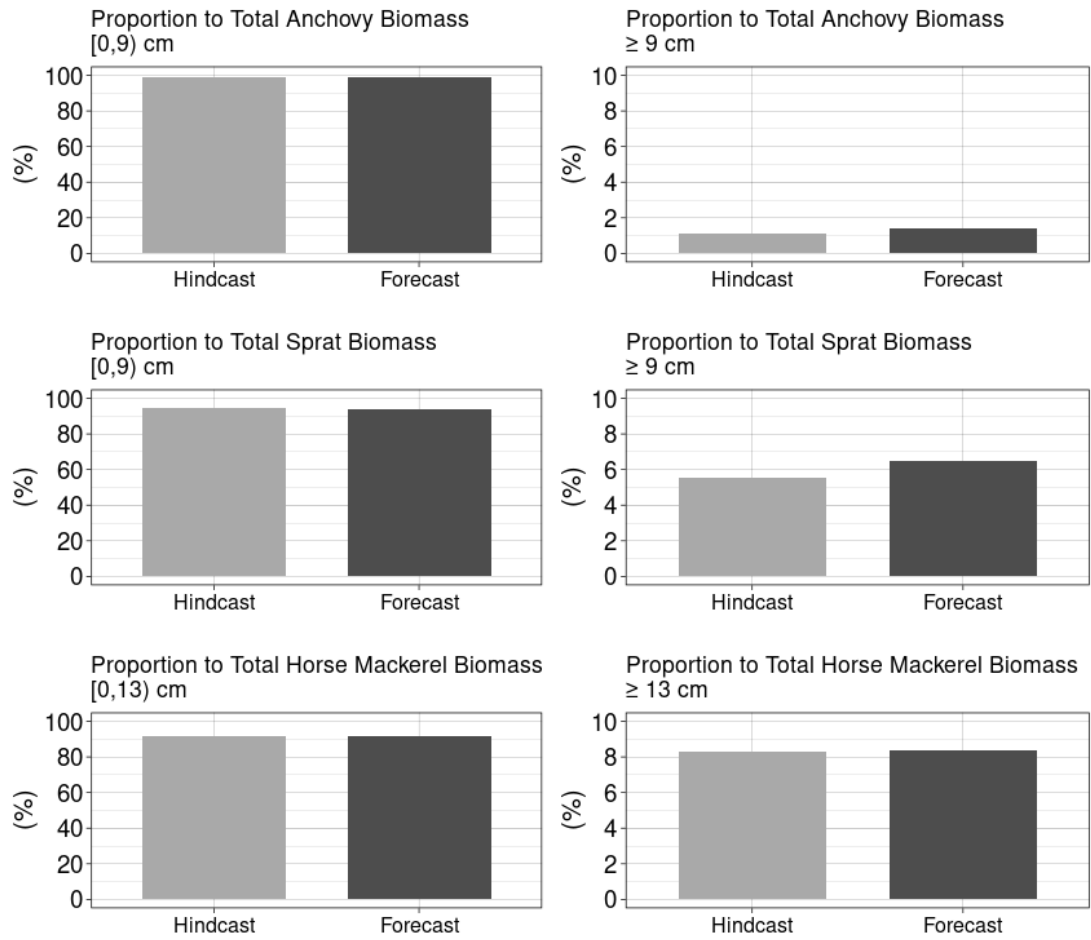


Figure 22. Proportions of the biomasses in size classes to the total biomasses of anchovy, sprat, and horse mackerel over 15 years within different size-classes for hindcast (2000–2014, light-gray bars) and forecast (2086–2100, dark-gray bars) scenarios.

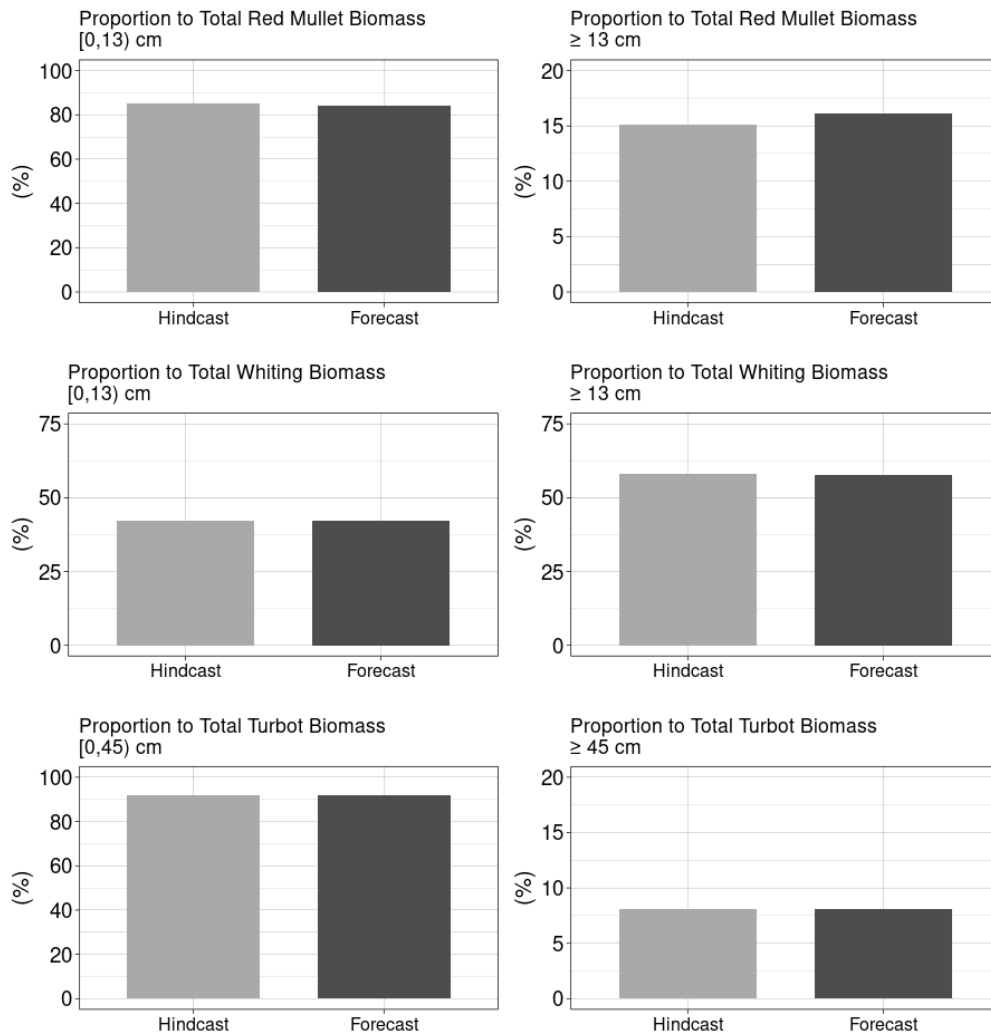


Figure 23 Proportions of the biomasses in size classes to the total biomasses of red mullet, whiting and turbot over 15 years within different size-classes for hindcast (2000–2014, light-gray bars) and forecast (2086–2100, dark-gray bars) scenarios.

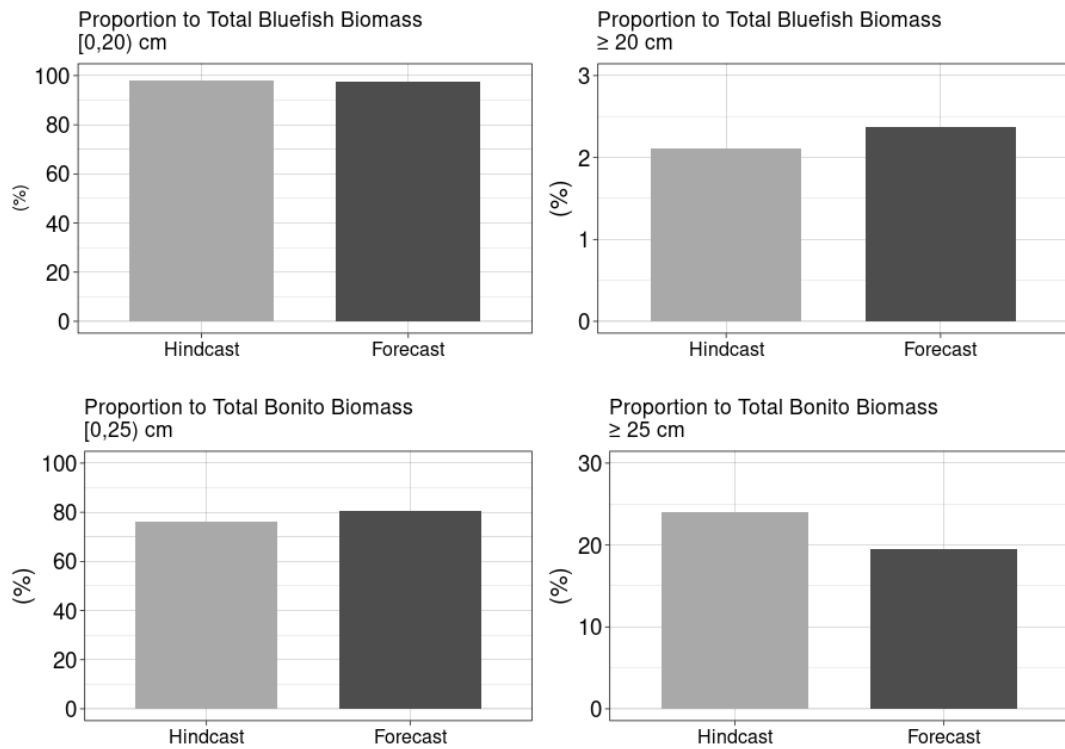


Figure 24 Proportions of biomasses in size classes to the total biomass of bluefish and bonito over 15 years within different size-classes for hindcast (2000–2014, light-gray bars) and forecast (2086–2100, dark-gray bars) scenarios.

The proportion of total biomass for all species across size classes revealed a slight decrease of 2.3% in the smallest size class (<10 cm). The size classes of 10-20 cm and 20-30 cm were projected to increase by 20.8% and 20.1%, respectively. No substantial difference was observed in the proportions of biomass for the 30-40 cm size class. The proportions of biomass for the largest size class (>40 cm) showed a decline of 22.4% by the end of the 21st century (Figure 25).

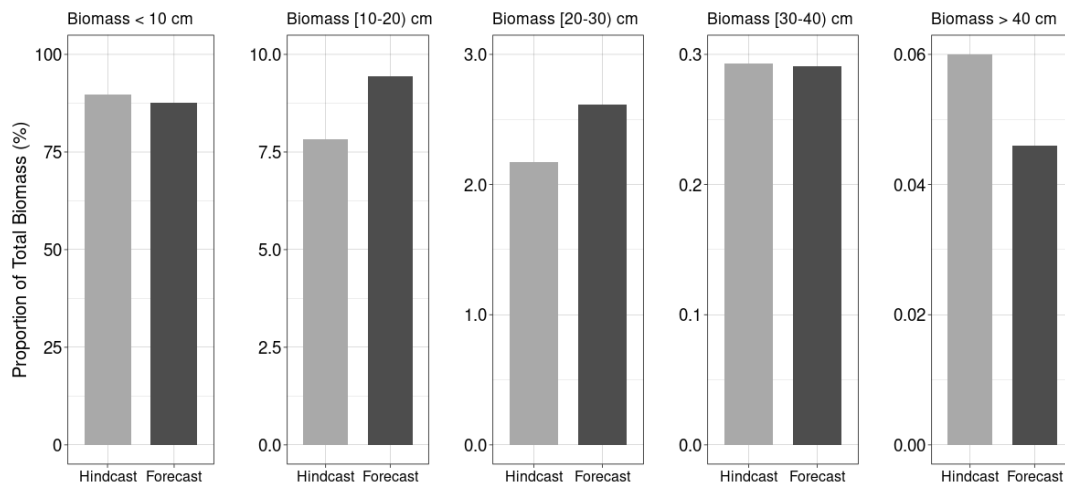


Figure 25. Proportions of biomasses in size classes to the total biomasses over 15 years within different size-classes for hindcast (2000–2014, light-gray bars) and forecast (2086–2100, dark-gray bars) scenarios.

### 3.4 Spatial Distributions

In Figures 26 and 27, the spatial distributions of simulated biomass for the hindcast and forecast scenarios were presented, respectively. The results indicated that anchovy populations were primarily distributed in the southeast and northwest regions for both scenarios. Both sprat and horse mackerel were spread across the entire area, with a dominant presence in the western parts of the region in the hindcast and the central parts of the region in the forecast scenario. For the demersal group, red mullet, whiting, and turbot, a widespread distribution was observed in the north and along the western coasts. Larger pelagic species, such as bluefish and bonito, predominantly occupy the southern Black Sea, with a particularly strong presence in the southwest.

When comparing the scenarios in Figure 28, a widespread increase in biomass across the entire region was anticipated for the pelagic group in the future. Anchovy, bluefish, and bonito were expected to spread throughout the entire region, while sprat

and horse mackerel were projected to increase mainly in the central and eastern parts. As for the demersal group, an increase in biomass was observed in the north and along almost all coastal areas.

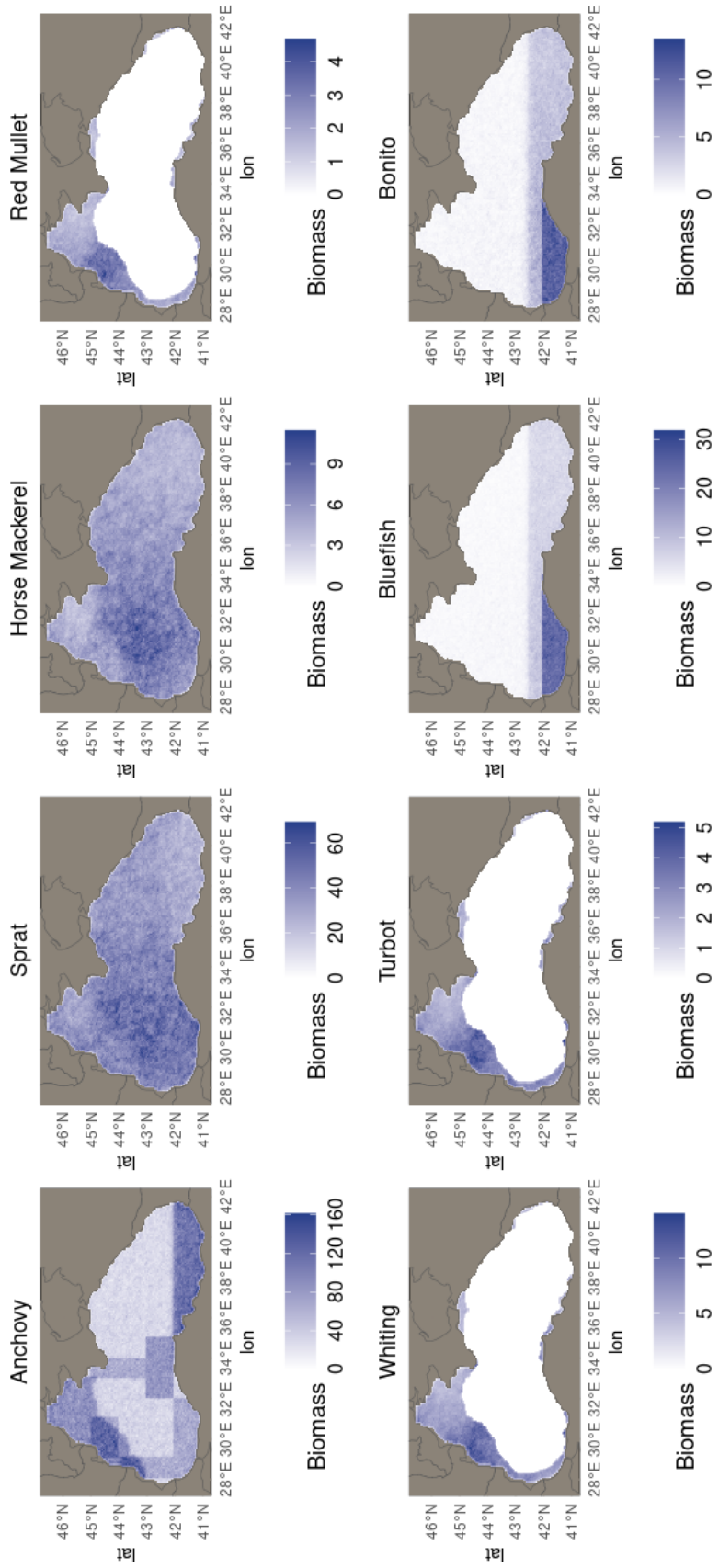


Figure 26. The spatial distribution of average biomass obtained from 10 simulation replicates for the hindcast scenario.

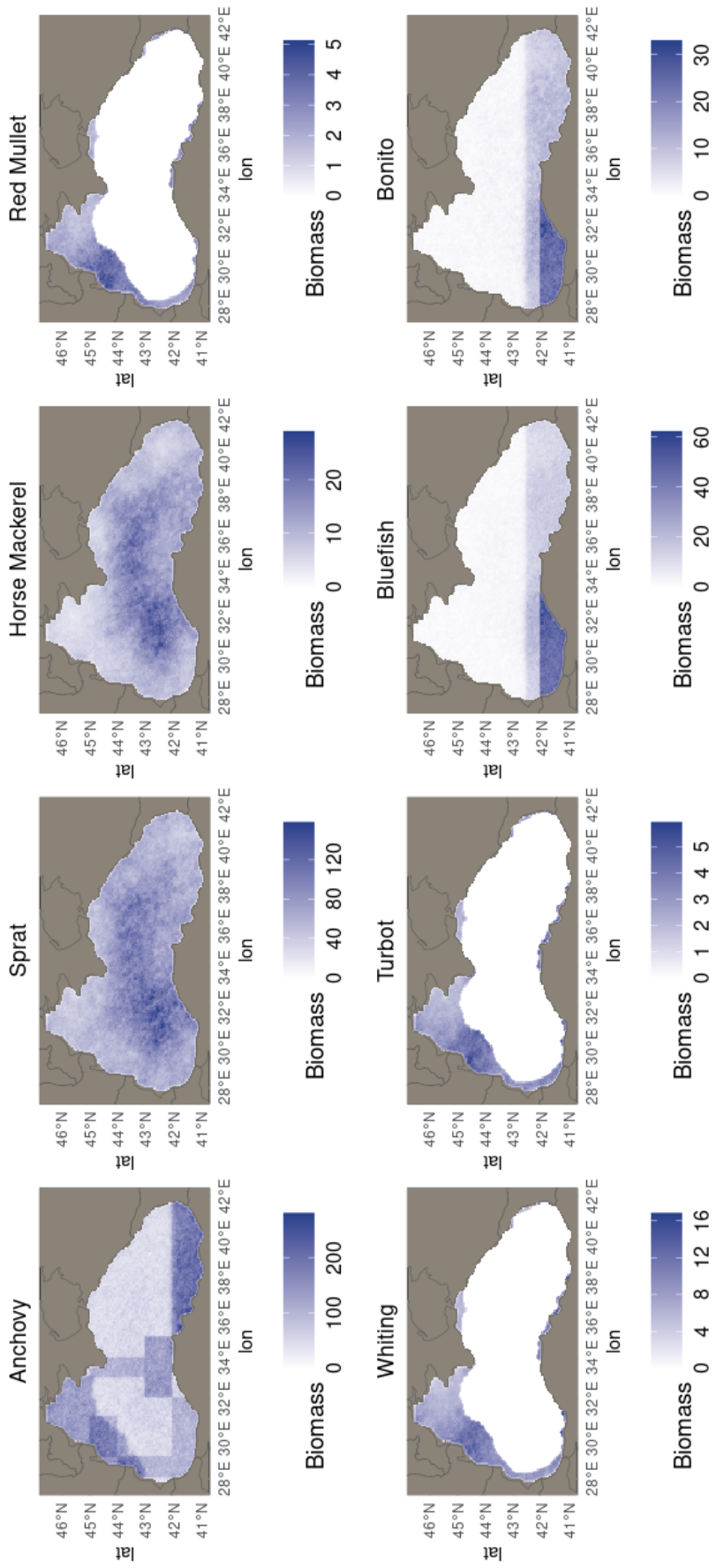


Figure 27. The spatial distribution of average biomass obtained from 10 simulation replicates for the forecast scenario.

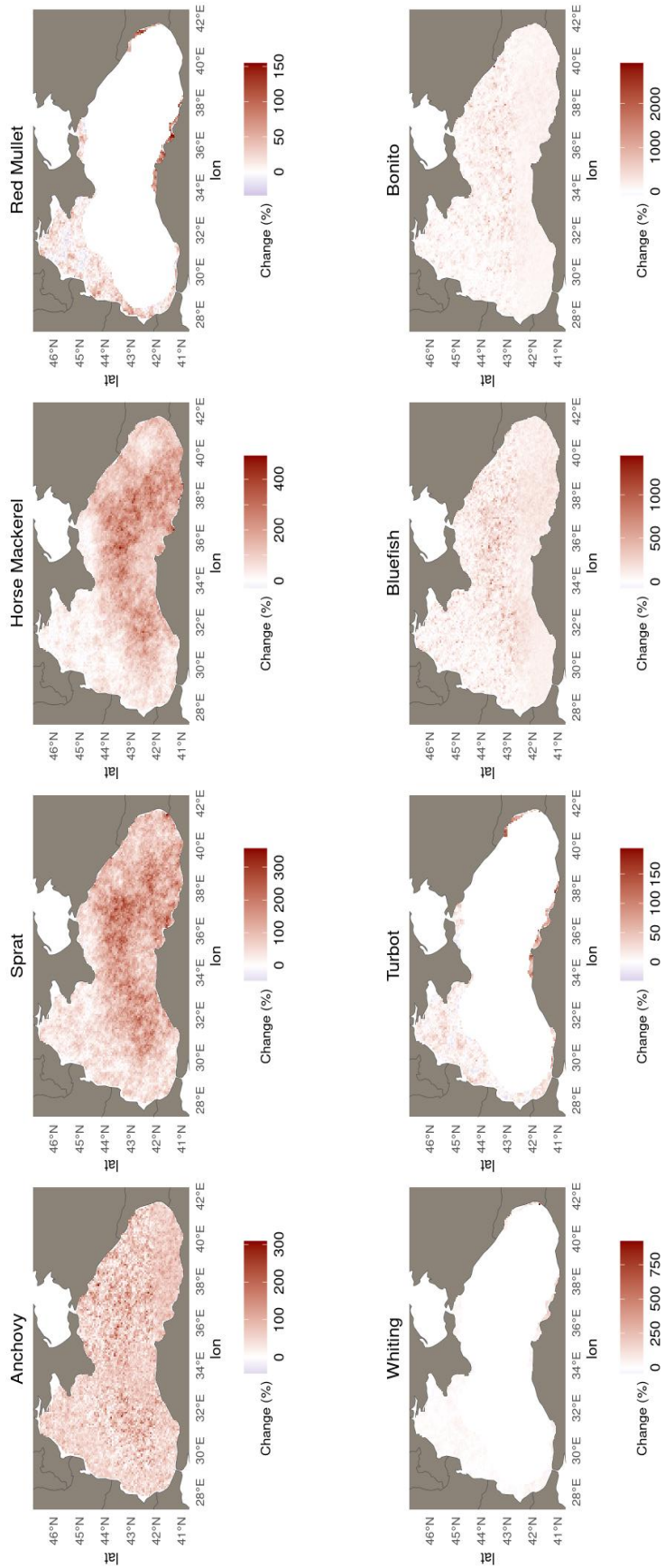


Figure 28. The change in spatial distribution of average biomass between the hindcast and forecast scenarios.



## CHAPTER 4

### DISCUSSION

The principal objective of this study was to enhance our understanding of the potential impact of future climate variation on eight economically significant fish species in the Black Sea. The findings of this study revealed two key insights. First, the projected increase in fish biomasses may be driven by the increases in the biomasses of lower-trophic-level species under future climate scenarios. Second, the model predicted an overall increase in biomass across all size classes for all species, with smaller individuals dominating the system. Therefore, fisheries management for the Black Sea should prioritize recovering populations of larger size groups and promoting sustainable fishing practices. This holistic approach would ensure the productivity of the long-term fisheries.

#### 4.1 Model Representation

OSMOSE-BS results in the 2000–2014 period were compared to an earlier study, which was conducted with the same species by using Ecosim with Ecopath (EwE) (Salihoğlu et al., 2017). Based on the median biomass values of these species, some similarities and disparities were observed, such as the higher biomass of anchovy and the lower biomass of Mediterranean horse mackerel obtained in EwE (Figure 29). The different predictions could be because the models were based on different assumptions. OSMOSE has sized-based opportunistic predation based on spatial cooccurrence and size sufficiency, with an explicit representation of the life cycle, whereas the earlier model used predetermined species-based diets. Corresponding to the difference in linkage between species (Figure 30), OSMOSE had higher prey-predator interactions, implying that higher opportunism led to higher responses to changes. Furthermore, OSMOSE involves 2-dimensional distribution maps of

species, varying based on age and season; however, EwE lacks spatialization, which means it does not account for prey-predator interactions in terms of their spatial distribution and movements. Therefore, OSMOSE may provide a more comprehensive understanding of ecosystem dynamics and capture prey-predator interactions in a spatial context, which leads to a more accurate assessment of management strategies for fisheries.

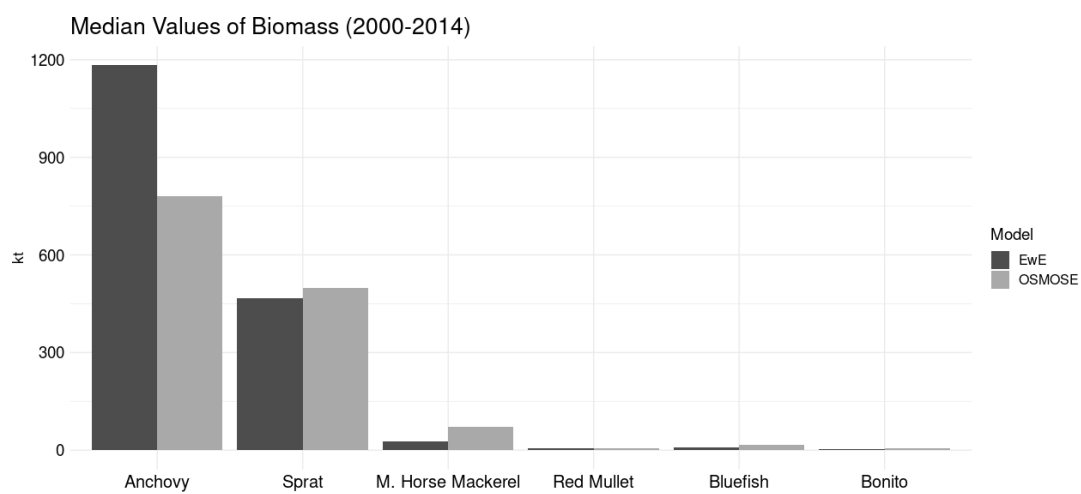
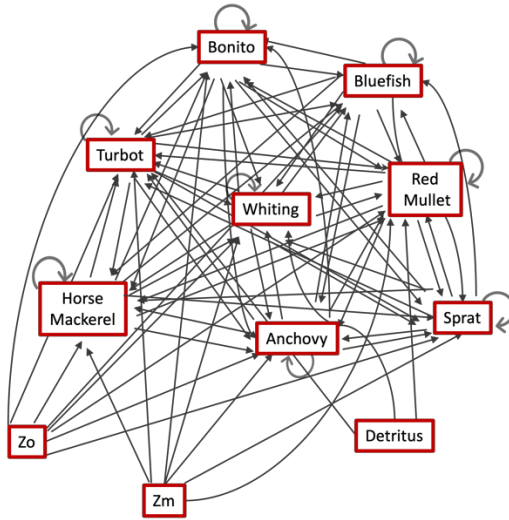


Figure 29. Median biomass values in the 2000–2014 period for OSMOSE-BS and EwE (Salihoğlu et al., 2017).

OSMOSE-BS



EwE

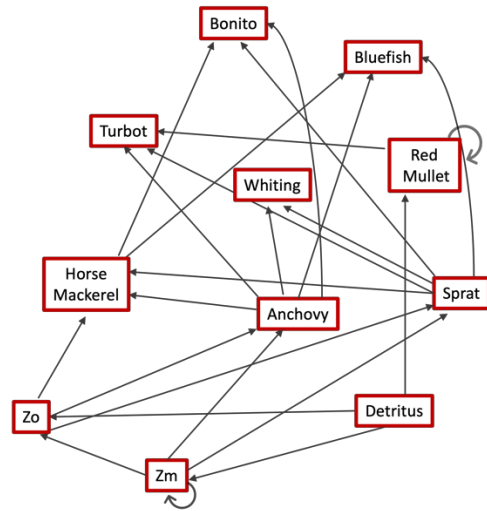


Figure 30. Schematic diagram of food web diet representations for OSMOSE-BS and EwE (adapted from Salihoğlu et al., 2017). The arrow represents the flow of prey-predator interactions. Zo and Zm represent mesozooplankton and microzooplankton, respectively. The model groups shown in EwE were selected to correspond to species in OSMOSE.

## 4.2 Model Validation and Skills

The characteristics of the OSMOSE-BS model simulation results were compared to the observed biomasses, catches, and mean sizes at catch data. To ensure the accuracy of the model outputs, a calibration process was initiated that involved adjusting six key parameters. However, the initial calibration did not yield results closely aligned with the reference data for both biomass and catch. Subsequently, modifications were made to four parameters: plankton accessibility for each plankton group, fishing mortality rate, maximum ingestion rate, and recruitment size parameters, to achieve a better fit for biomass and catch. Following the calibration and parameter adjustments, noteworthy patterns in the validation results were observed.

For biomass comparison with stock assessment estimates, some discrepancies were observed. Bluefish and bonito were not considered in the biomass validation because of the lack of observed biomass data. With the exception of red mullet, the model slightly overestimated biomass for all species when compared to the stock assessment predicted biomass values in most years. This can create uncertainty in biomass results in future scenarios and lead to higher biomass values than it should be. However, low biomass estimates of red mullet may indicate a need for careful consideration in future biomass predictions. These discrepancies could lead to an underestimation of the risks associated with climate change impacts.

Furthermore, the model displayed catch projections consistent with the statistical catch data, indicating its ability to provide reliable predictions for catches. However, underestimation of anchovy catch, which is the main unreported species based on its high catch proportion (Ulman et al., 2013), was observed; thus, catch of anchovy values may actually be much higher. However, an overestimation of whiting, which has often been caught by sprat fisheries in the Black Sea (Raykov et al., 2008), was observed. Therefore, the overestimation value in the model result may slightly offset this situation, and the future may not appear to have as much uncertainty for whiting. Overall, it is important to note that illegal, unreported, and unregulated (IUU) fishing was common in the Black Sea, with turbot serving as the main target of this illegal fishery (Öztürk, 2013). All modeled species in this study were involved in unreported fisheries in the Black Sea (Keskin et al., 2015; Ulman et al., 2013, 2015). Therefore, even if species catch projections were consistent with statistical catch data in general, they may actually have higher values, especially for anchovy.

For the mean size at catch validation, the model underestimated mean sizes for turbot and bonito compared to observed data. Conversely, it significantly overestimated whiting's mean size. Although the Spearman's rank correlation coefficient of 0.74 suggests a relatively strong linear association between the model and observations, these discrepancies emphasized the necessity for further investigation into the

model's representation of fish size, which is important not only for validation but also for fisheries management (e.g., size limits, maturity size).

### **4.3 Evaluation of Model Results**

#### **i) Biomass and Catch Projections**

The individual-based OSMOSE-BS model presented in this study projected an increase in biomass and catch values for all higher-trophic-level species by the end of the 21st century. The increases were linked to the projected increases in biomasses of lower-trophic-level species by the global climate model IPSL-CM6A-LR. The increases in zooplankton and detritus were linked to the increase in primary production. This implied bottom-up control of the zooplankton group by primary production and bottom-up control of the higher trophic levels by zooplankton. The increase in zooplankton biomass in this study was consistent with the study conducted by Moullec et al. (2019), which projected an increase of 1% for mesozooplankton and 4% for microzooplankton biomass in the Mediterranean Sea by the end of the century under the IPCC RCP8.5 scenario.

In contrast to the predictions for lower-trophic-level species in this study, no significant changes in mesozooplankton and microzooplankton biomass were observed, despite an increase in net primary production until 2100 in the Black Sea using a regional model, BIMS-ECO (Akoğlu et al., 2013; Cannaby et al., 2015). This disparity may be because global-scale models do not accurately represent unique local environmental conditions on smaller scales (Feser et al., 2011). Therefore, it is important to implement local high-resolution climate models in future research. These models can provide a more detailed and accurate representation of the relationship between climate forcing and ecosystem responses in regional ecosystems.

The greatest increases in biomasses were observed in pelagic fish species. This might be attributed mainly to the increased availability of food, as they primarily fed on smaller pelagic fish and mesozooplankton, which showed a significant increase (103.85%). Among the small pelagic fish species modeled in this study, anchovy biomass was projected to increase by 60%, sprat by 85%, and horse mackerel by 105%. The relatively lower increase in anchovy might be attributed to the higher fishing mortality rate of anchovies compared to others. This study observed a drastic decline in the biomasses of small pelagic species after 2090. This decline may be linked to the slight decrease predicted in microzooplankton biomass. Interestingly, although an increase in mesozooplankton biomass was also observed in the same year, a fluctuation in microzooplankton affected the abundance of small fish species, which may indicate that the system is dominated by smaller fish in the populations of pelagic species that prefer microzooplankton as the primary food source. Furthermore, increases in starvation mortality rates were observed across all fish species except anchovy in that year (Appendices B, Figure B.2). Additionally, an increase in the predation mortality rate of sprat after 2090 may have also contributed to the decline in sprat's biomass (Appendices B, Figure B.1).

Furthermore, small pelagic species had a slightly modest increase compared to larger pelagic ones. Within the framework of the prey-predator relationship, increasing the biomass of large pelagic species might cause higher predation pressure on small pelagic species, which may lead to a decrease or increase to a lesser extent of small pelagic biomass. However, this model cannot catch such changes; in fact, horse mackerel had a higher increase than bluefish. Therefore, the model may underestimate the potential impact of prey-predator interactions. Thus, small pelagic species stocks may be more affected than predicted.

The comparatively modest increase observed in demersal fish species such as red mullet, whiting, and turbot could be attributed to their lower plankton intake rates, as depicted in the model. Additionally, the mean predation mortality rates of red mullet and turbot were observed to increase in the future (Appendices B, Table B.1).

Hence, while red mullet and whiting were predators of smaller species, the increase in the biomass of pelagic predatory fish species may have placed increased predatory pressure on them. These results were consistent with a study by Moullec et al. (2019) in the Mediterranean Sea, which predicted a relatively small increase of 3% in the biomass of demersal fish compared to a 25% increase in the biomass of pelagic fish species by the end of this century in the Mediterranean Sea under the IPCC RCP 8.5 scenario.

In the future scenario, an increase in biomass was noted in the entire area where fish species were described. Notably, an increase in biomass for small pelagic species, particularly sprat and horse mackerel, was observed in the central and eastern parts. This increase may be directly associated with the conspicuous rise in biomass at the lower trophic levels within the central and eastern parts of the Black Sea (Appendices C, Figure C.1).

Simulated catches for all species were projected to increase by the end of the 21st century, reflecting the trends simulated for biomasses. The most significant increases in catches were simulated for pelagic species, which also showed the most substantial increases in biomasses. This trend was subsequently observed in catches of the demersal fish group. OSMOSE-BS projections on catch changes aligned with the trends reported by Moullec et al. (2019). They noted a more pronounced increase of 9% in pelagic catches and a relatively smaller increase of about 2% in demersal fish. However, maintaining a constant fishing mortality rate in the whole region in both scenarios may yield results that diverge from actual real-world conditions. Consequently, incorporating varied fishing scenarios, in conjunction with future climate change scenarios, into the model is likely to yield more realistic estimates of fish catch values.

#### ii) Sized-Based Projections

An increase in biomass was generally observed in all size classes. Increases in biomasses for small pelagic species within the 1-3 cm size range may be attributed

to an increase in the availability of food, potentially due to the increases in lower-trophic-level species and a lack of fishing pressure on these groups. The reason for the relatively lower fractional change for demersal fish compared to pelagic species according to their sizes possibly because of relatively less accessibility rate to plankton. For bonito smaller than 11 cm, the increase may similarly be linked to food abundance.

Across both historical and future climate scenarios, the fish assemblage was dominated by smaller individuals, contributing over 75% of the total biomasses of the populations with the exception of whiting. Notably, smaller and medium-sized species held a greater proportional contribution to total biomass compared to larger size classes. This dominance of smaller individuals coincided with the increase in biomass of lower trophic level species. This pattern might be attributable to the different responses of fish size classes to environmental changes. Species of smaller size typically exhibit greater variations in biomass as a reaction to these changes than larger ones with slower turnover rates (Brown et al., 2010; Pennino et al., 2020). Interestingly, whiting deviated from this trend, with a higher proportion of larger individuals simulated. This may be explained by a relatively lower fishing mortality rate for whiting compared to other species. The proportion of total biomass in OSMOSE-BS projections aligned with changes reported by Moullec et al. (2019). They observed a 7% increase in the proportion of biomass for the smaller size class (10–20 cm) and a 15% decrease for the largest size class (> 40 cm).

#### **4.4 Limitations and Future Work**

End-to-end ecosystem models are useful tools for representing complex ecosystems in their entirety. Despite the comprehensiveness of ecosystem dynamics and interactions, abstracting these dynamics and interactions to develop an ecosystem model using parameters and mathematical expressions inevitably brings a plethora of uncertainties (Hill et al., 2007).



In this study, the OSMOSE-BS model was used to describe eight fish species of high economic value by integrating a vast array of life cycle parameters and information from scientific literature, databases, and stock assessment reports. The challenges of data availability, including the lack of stock assessments and accessibility were significant obstacles to the development, parameterization, and validation of ecosystem models (Coll et al., 2013). Therefore, the development of the OSMOSE model for the Black Sea and the simplification of the model's ecosystem led to some constraints in this study.

The majority of data utilized to parameterize the model were collected from the study area that corresponded to the period of the hindcast scenario; however, certain parameters for species with limited data (bluefish and bonito) were obtained from adjacent ecosystems (the Sea of Marmara). Therefore, validation of the simulated biomass values could not be provided for these species. This can lead to uncertainty in estimations of bluefish and bonito in the Black Sea and may influence the predictions of other species interacting with them, either as prey or predators.

In this study, temperature variations were constrained only by lower trophic levels. Consequently, the temperature preferences of fish species were overlooked, potentially introducing uncertainty in predictions of biomass changes. For instance, sprat, a species that prefers cold water, showed a higher increase in biomass compared to its warm-water-preferring competitors, such as anchovy. By excluding these preferences, this study may have underestimated the potential impact of temperature variation on fish populations. Therefore, a modest increase in sprat biomass could be observed in the future compared to that of anchovy. This highlights the need for further research to incorporate species-specific temperature preferences into future prediction and management strategies.

Fish populations might also react to climate-related stress through physiological adaptations. Morell et al. (2023) developed a bioenergetic model for OSMOSE to represent the physiological responses of high trophic levels for changes in temperature and oxygen levels in the future. To delineate the alterations that could

either lessen or amplify the effects of climate change considering the life cycle of fishes, future studies with the OSMOSE-BS model employ evolutionary and bioenergetic modules that represent the energetic trade-off between growth and reproduction.

Moreover, the fishing parameters assumed a uniform spatial distribution and remained constant throughout the year. However, this approach might not accurately represent the actual fishing dynamics in the Black Sea. The uniformity assumed in the model did not account for regional variations in fishing activities where different countries implement various fishing management practices, such as closed seasons and areas and minimum landing sizes. Consequently, this could lead to oversimplification of the varied fishing pressures experienced in the different parts of the Black Sea. Spatially explicit fishery dynamics in different regions should be noted in future studies to improve the representation of the effects of the variability in fishing efforts on the ecosystem, in addition to climate change.

#### **4.5 Potential uses of OSMOSE-BS**

The fish species modeled in this study, which exhibited increases in both biomass and catch levels due to climate change, were critical flagship species for Black Sea fisheries. Therefore, the model findings could be an indicator for new opportunities for future Black Sea fisheries. The projected increase in fish stocks may elevate Black Sea countries to become significant players in the global fish market through expanding the fishing industry, improving traditional fishing activities, and potentially attracting investment in fishing infrastructure, technology, and endeavors. Expanding fishing-affected sectors may create considerable job opportunities, extending beyond fishing to include processing, marketing, and distribution. Thus, this condition may positively impact local economies and strengthen economic security in Black Sea countries.

The findings of this study indicated the widespread dominance of smaller individuals within the majority of fish populations in both scenarios. The results showed that the proportion of biomass for fish smaller than 10 cm was 89.7% in the hindcast scenario, while it was observed to be 87.6% in the future scenario. Despite the possibility that larger pelagic exert a higher predation pressure on smaller ones, the difference between the two scenarios was quite small. Therefore, these results could potentially indicate unsustainable fishing practices during both the periods. According to recent stock assessments in Turkish waters, most of species were subjected to overfishing (Demirel et al., 2020). As an examination of the situation of Black Sea fishing so far, overfishing has emerged as one of the key factors influencing various regimes (Akoglu, 2023). In fact, by 2019, the Food and Agriculture Organization (FAO) reported that 63.4% of fish stocks in the Mediterranean and Black Sea were being exploited at unsustainable levels (FAO, 2022). Furthermore, only 1.4% of anchovy, which is the most commercially important target species in the Black Sea, was projected to constitute a larger size class in the future. Therefore, it is crucial to prioritize sustainable fisheries and ecosystem management practices to ensure long-term viability in the Black Sea. Management strategies should focus on increasing the proportions of large-sized individuals in the populations, considering that the proportions of fish belonging to larger size groups were 8% in most populations. In that case, properly managed and implemented fishing quotas across all Black Sea countries may help increase proportion of larger individuals within fish populations. This approach will not only help maintain healthier interactions in the food-web, but also contribute to the formation of more productive stocks, which will be important for Black Sea fisheries.

This study was the first attempt to investigate the long-term projections of fish stocks in the Black Sea under climate change. Therefore, this study could serve as a tool for stakeholders to develop climate-adaptive fishing strategies for future. While these findings may offer valuable opportunities for future research and development, it is crucial to interpret them considering the limitations and uncertainties of the model, such as constant fishing mortality and the lack of physiological responses of fish

species to temperature variations. When critically evaluating model outcomes, it is essential to consider potential alterations in fishery dynamics and their implications for fish population.

## CHAPTER 5

### CONCLUSION

Until now, Black Sea model studies often employed a mass-balanced approach, concentrating more on the whole ecosystem structure in the Black Sea. Furthermore, the long-term effects of climate change on the Black Sea ecosystem and fish populations have not been studied extensively. To address this gap, this pioneering study aimed to comprehensively integrate the impacts of climate change on eight economically significant fish species, anchovy, sprat, horse mackerel, red mullet, whiting, turbot, bluefish, and bonito, by the end of the 21st century. This study showcased the first application of a size-based opportunistic approach in the Black Sea using an individual-based model, OSMOSE, under hindcast (2000-2014) and future climate scenarios, SSP3.70 (2086-2100), which enhanced our understanding of ecosystem dynamics and providing an innovative tool for future ecological forecasting.

OSMOSE, an end-to-end modelling framework, was required to couple to a lower trophic level as a resource for higher trophic level species. Therefore, mesozooplankton, microzooplankton, and detritus data were incorporated from the global climate model (IPSL-CM6A-LR). By the end of this century, an increase was simulated for all lower trophic level species, with a significant increase of 103.8% in mesozooplankton.

The projected increase in lower-trophic-level species was reflected in higher-trophic-level species, increasing both biomass and catch values in the future. Moreover, an increase in biomass distribution by size class was observed in all size classes of fish species, particularly in smaller size classes of small pelagic species. Furthermore, smaller individuals were projected to dominate the populations of fish species in the ecosystem, contributing over 80% of their total biomass, with the exception of

whiting in the future. In addition, smaller and medium-sized species had a greater proportional contribution to total biomass compared to larger size classes. The dominance of smaller individuals was an indicator of unsustainable fishing strategy in the black sea. Furthermore, the larger anchovy size group was found to constitute only 1.4% of the total anchovy biomass in the future. Hence, it is crucial to concentrate on replenishing the larger-sized individuals in the black sea fishery management. However, acknowledging the uncertainties of the model in this study is necessary, including the assumption of constant fishing mortality and the absence of consideration for the physiological responses of fish species to climatic fluctuations. Future studies should address these uncertainties of the model to enhance its predictive accuracy and reliability.

## REFERENCES

- Akoglu, E. (2023). Ecological indicators reveal historical regime shifts in the Black Sea ecosystem. *PeerJ*, *11*, e15649.
- Akoglu, E., Salihoglu, B., Libralato, S., Oguz, T., & Solidoro, C. (2014). An indicator-based evaluation of Black Sea food web dynamics during 1960–2000. *Journal of Marine Systems*, *134*, 113-125.
- Arai, M. N. (2001). Pelagic coelenterates and eutrophication: A review. In *Jellyfish Blooms: Ecological and Societal Importance: Proceedings of the International Conference on Jellyfish Blooms, held in Gulf Shores, Alabama, 12–14 January 2000* (pp. 69-87). Springer Netherlands.
- Ateş, C., Cengiz Deval, M., & Bök, T. (2008). Age and growth of Atlantic bonito (*Sarda sarda* Bloch, 1793) in the Sea of Marmara and Black Sea, Turkey. *Journal of Applied Ichthyology*, *24*(5), 546-550.
- Avsar, D. (1995). Population parameters of sprat (*Sprattus sprattus phalericus* Risso) from the Turkish Black Sea coast. *Fisheries research*, *21*(3-4), 437-453.
- Avşar, D. (1999). Identification of turbot (*Scophthalmus maximus*) stock along the Turkish Black Sea coast. *Turkish Journal of Zoology*, *23*(5), 207-214.

- Avsar, D., & Bingel, F. (1994). A preliminary Study on the Reproductive Biology of the Sprat (*Sprattus sprattus phalericus* (Risso, 1826)) in Turkish Waters of the Black Sea. *Tr. J. of Zoology*, 18, 77-85.
- Aydın, M., & Karadurmuş, U. (2012). Age, growth, length-weight relationship and reproduction of the Atlantic horse mackerel (*Trachurus trachurus* Linnaeus, 1758) in Ordu (Black Sea). *Ordu Üniversitesi Bilim ve Teknoloji Dergisi*, 2(2), 68-77.
- Aydın, M., & Karadurmuş, U. (2013). An investigation on age, growth and biological characteristics of red mullet (*Mullus barbatus ponticus*, Essipov, 1927) in the Eastern Black Sea.
- Bal, H., Yanık, T., & Türker, D. (2015). Length-Weight and Length-Length Relationships of The Bluefish *Pomatomus saltarix* (Linnaeus. 1766) Population in the South Marmara Sea of Turkey. *Alinteri Journal of Agriculture Sciences*, 29(2).
- Boucher, O., Servonnat, J., Albright, A. L., Aumont, O., Balkanski, Y., Bastrikov, V., ... & Vuichard, N. (2020). Presentation and evaluation of the IPSL-CM6A-LR climate model. *Journal of Advances in Modeling Earth Systems*, 12(7), e2019MS002010.
- Brierley, A. S., & Kingsford, M. J. (2009). Impacts of climate change on marine organisms and ecosystems. *Current biology*, 19(14), R602-R614.



- Brown, C. J., Fulton, E. A., Hobday, A. J., Matear, R. J., Possingham, H. P., Bulman, C., ... & Richardson, A. J. (2010). Effects of climate-driven primary production change on marine food webs: implications for fisheries and conservation. *Global Change Biology*, *16*(4), 1194-1212.
- Caddy, J. F., & Griffiths, R. C. (1990). Recent trends in the fisheries and environment in the General Fisheries Council for the Mediterranean (GFCM) area (No. 63). *Food & Agriculture Org.*
- Ceyhan, T., Akyol, O., Ayaz, A., & Juanes, F. (2007). Age, growth, and reproductive season of bluefish (*Pomatomus saltatrix*) in the Marmara region, Turkey. *ICES Journal of Marine Science*, *64*(3), 531-536.
- Chavez, F. P., Ryan, J., Lluch-Cota, S. E., & Niquen C, M. (2003). From anchovies to sardines and back: Multidecadal change in the Pacific Ocean. *Science*, *299*(5604), 217-221.
- Christensen, V., & Pauly, D. (Eds.). (1993). Trophic models of aquatic ecosystems (Vol. 26). WorldFish.
- Christensen, V., & Walters, C. J. (2004). Ecopath with Ecosim: Methods, capabilities and limitations. *Ecological Modelling*, *172*(2-4), 109-139.
- Chust, G., Allen, J. I., Bopp, L., Schrum, C., Holt, J., Tsiaras, K., ... & Irigoien, X. (2014). Biomass changes and trophic amplification of plankton in a warmer ocean. *Global Change Biology*, *20*(7), 2124-2139.

- Coll, M., Cury, P., Azzurro, E., Bariche, M., Bayadas, G., Bellido, J. M., ... & Workshop Participants. (2013). The scientific strategy needed to promote a regional ecosystem-based approach to fisheries in the Mediterranean and Black Seas. *Reviews in fish biology and fisheries*, 23, 415-434.
- Cury, P. M., Shin, Y. J., Planque, B., Durant, J. M., Fromentin, J. M., Kramer-Schadt, S., ... & Grimm, V. (2008). Ecosystem oceanography for global change in fisheries. *Trends in Ecology & Evolution*, 23(6), 338-346.
- Daskalov, G. M. (2002). Overfishing drives a trophic cascade in the Black Sea. *Marine Ecology Progress Series*, 225, 53-63.
- Daskalov, G.M. (2003). Long-term changes in fish abundance and environmental indices in the Black Sea. *Mar. Ecol., Prog. Ser* 255, 259–270.
- Daskalov, G. M., Demirel, N., Ulman, A., Georgieva, Y., & Zengin, M. (2020). Stock dynamics and predator–prey effects of Atlantic bonito and bluefish as top predators in the Black Sea. *ICES Journal of Marine Science*, 77(7-8), 2995-3005.
- Demirel, N., & Yüksek, A. (2013). Reproductive biology of *Trachurus mediterraneus* (Carangidae): a detailed study for the Marmara–Black Sea stock. *Journal of the marine biological Association of the United Kingdom*, 93(2), 357-364.

- Demirel, N., Zengin, M., & Ulman, A. (2020). First large-scale Eastern Mediterranean and Black Sea stock assessment reveals a dramatic decline. *Frontiers in Marine Science*, 7, 103.
- Demirel, N., Akoglu, E., & Yıldız, T. (2023). Shifts in the pelagic fishery dynamics in response to regional sea warming and fishing in the Northeastern Mediterranean. *Regional Environmental Change*, 23(4), 141.
- Duboz, R., Versmisse, D., Travers, M., Ramat, E., & Shin, Y. J. (2010). Application of an evolutionary algorithm to the inverse parameter estimation of an individual-based model. *Ecological modelling*, 221(5), 840-849.
- Erdoğan-Sağlam, N.E. & Sağlam, C. (2013). Age, growth and mortality of anchovy *Engraulis encrasicolus* in the south-eastern region of the Black Sea during the 2010-2011 fishing season. *J. Mar. Biol. Assoc. United Kingdom*, 93, 2247–2255.
- Eryilmaz, L., & Dalyan, C. (2015). Age, growth, and reproductive biology of turbot, *Scophthalmus maximus* (Actinopterygii: Pleuronectiformes: Scophthalmidae), from the south-western coasts of Black Sea, Turkey. *Acta ichthyologica et piscatoria*, 45(2), 181-188.
- FAO. (2014). *The State of World Fisheries and Aquaculture 2014*. Rome. 223 pp.
- FAO. (2022). *The State of World Fisheries and Aquaculture 2022. Towards Blue Transformation*. Rome, FAO. <https://doi.org/10.4060/cc0461en>

- Fromentin, J. M., & Planque, B. (1996). Calanus and environment in the eastern North Atlantic. II. Influence of the North Atlantic Oscillation on *C. finmarchicus* and *C. helgolandicus*. *Marine Ecology Progress Series*, 134, 111-118.
- Fu, C., Perry, R. I., Shin, Y. J., Schweigert, J., & Liu, H. (2013). An ecosystem modelling framework for incorporating climate regime shifts into fisheries management. *Progress in Oceanography*, 115, 53-64.
- Fulton, E.A., Fuller, M., Smith, A.D.M., Punt, A.E. (2005). Ecological Indicators of the Ecosystem Effects of Fishing: Final Report. *Australian Fisheries Management Authority Report, R99/1546*. 239 pp.
- Fulton, E. A. (2010). Approaches to end-to-end ecosystem models. *Journal of Marine Systems*, 81(1-2), 171-183.
- Gaines, S. D., Costello, C., Owashi, B., Mangin, T., Bone, J., Molinos, J. G., ... & Ovando, D. (2018). Improved fisheries management could offset many negative effects of climate change. *Science advances*, 4(8), eaao1378.
- Garrabou, J., Coma, R., Bensoussan, N., Bally, M., Chevaldonné, P., Cigliano, M., ... & Cerrano, C. (2009). Mass mortality in Northwestern Mediterranean rocky benthic communities: effects of the 2003 heat wave. *Global change biology*, 15(5), 1090-1103.

Genc, Y. (2000). Türkiye nin Doğu Karadeniz Kıyılarındaki Barbunya (*Mullus barbatus ponticus*, Ess. 1927) Balığının Biyoeolojik Özellikleri ve Populasyon Parametreleri. Fen Bilimleri Enstitüsü, Bal. Tekn. Müh. Anabilim Dalı, Trabzon. İşmen, A. (2002). A preliminary study on the population dynamics parameters of whiting (*Merlangius merlangus euxinus*) in Turkish Black Sea coastal waters. *Turkish Journal of Zoology*, 26(2), 157-166.

GFCM. 2022. Stock Assessment Form Small Pelagics. <https://www.fao.org/gfcm/data/safs>

Gislason, H., and Helgason, T. 1985. Species interaction in assessment of fish stocks with special application to the North Sea. *Dana*, 5: 1–44.

Gordina, A.D. (1996). On bluefish (*Pomatomus saltatrix* L.) spawning in the Black Sea. *Marine and Freshwater Research*, 47(2), 315-318

Gruber, N. (2011). Warming up, turning sour, losing breath: ocean biogeochemistry under global change. *Philosophical Transactions of the Royal Society A: Mathematical, Physical and Engineering Sciences*, 369(1943), 1980-1996.

Gucu, A.C. (2002). Can overfishing be responsible for the successful establishment of *Mnemiopsis leidyi* in the Black Sea? *Estuarine, Coastal and Shelf Science*, 54, 439-451.

- Halouani, G., Lasram, F. B. R., Shin, Y. J., Velez, L., Verley, P., Hattab, T., ... & Romdhane, M. S. (2016). Modelling food web structure using an end-to-end approach in the coastal ecosystem of the Gulf of Gabes (Tunisia). *Ecological Modelling*, 339, 45-57.
- Hill, S. L., Watters, G. M., Punt, A. E., McAllister, M. K., Quéré, C. L., & Turner, J. (2007). Model uncertainty in the ecosystem approach to fisheries. *Fish and Fisheries*, 8(4), 315-336.
- Hoegh-Guldberg, O., Cai, R., Poloczanska, E. S., Brewer, P. G., Sundby, S., Hilmi, K., ... & McKinnell, S. M. (2014). The ocean.
- Hoegh-Guldberg, O., Lovelock, C., Caldeira, K., Howard, J., Chopin, T., & Gaines, S. (2019). The ocean as a solution to climate change: five opportunities for action.
- IPCC. (2007). *Climate Change 2007: The Physical Science Basis. Contribution of Working Group I to the Fourth Assessment Report of the Intergovernmental Panel on Climate Change*. Cambridge University Press.
- Ivanov, L., & Beverton, R. J. H. (1985). The Fisheries Resources of the Mediterranean Part 2, Black Sea Stud.
- Ivanov, L. & Panayotova, M. (2001) Determination of the Black Sea anchovy stocks during the period 1968 – 1993 by Ivanov's combined method. *Proc Inst Oceanol Bulg Acad Sci*, 3,128–154.

- İBB. (2020). Deniz Balıkları. [online] Available at: <https://gida.ibt.istanbul/tarim-ve-su-urunleri-mudurlugu/deniz-baliklari.html> [Accessed Date 12/03/2020].
- İşmen, A. (2002). A preliminary study on the population dynamics parameters of whiting (*Merlangius merlangus euxinus*) in Turkish Black Sea coastal waters. *Turkish Journal of Zoology*, 26(2), 157-166.
- Kabel, K., Moros, M., Porsche, C., Neumann, T., Adolphi, F., Andersen, T. J., ... & Sinninghe Damsté, J. S. (2012). Impact of climate change on the Baltic Sea ecosystem over the past 1,000 years. *Nature Climate Change*, 2(12), 871-874.
- Kahraman, A. E., Göktürk, D., Yildiz, T., & Uzer, U. (2014). Age, growth, and reproductive biology of Atlantic bonito (*Sarda sarda* Bloch, 1793] from the Turkish coasts of the Black Sea and the Sea of Marmara. *Turkish Journal of Zoology*, 38(5), 614-621.
- Kalaycı, F., Samsun, N., Bilgin, S., & Samsun, O. (2007). Length-weight relationship of 10 fish species caught by bottom trawl and midwater trawl from the Middle Black Sea, Turkey. *Turkish Journal of Fisheries and Aquatic Sciences*, 7(1).
- Kasapoğlu, N. (2018). Age, growth, and mortality of exploited stocks: anchovy, sprat, Mediterranean horse mackerel, whiting, and red mullet in the southeastern Black Sea. *Aquatic Sciences and Engineering*, 33(2), 39-49.

- Keeling, R. F., Körtzinger, A., & Gruber, N. (2010). Ocean deoxygenation in a warming world. *Annual review of marine science*, 2, 199-229.
- Keskin, Ç., Ulman, A., Raykov, V., Daskalov, G. M., Zylich, K., Pauly, D., & Zeller, D. (2015). Reconstruction of fisheries catches for Bulgaria: 1950-2010.
- Kideys, A.E. (2002). Fall and rise of the Black Sea ecosystem. *Science*, 297,1482-1484.
- Konovalov, S. K., Murray, J. W., & Luther III, G. W. (2005). Black Sea Biogeochemistry. *Oceanography*, 18(2), 24-35.
- Köster, F. W., Möllmann, C., Hinrichsen, H. H., Wieland, K., Tomkiewicz, J., Kraus, G., ... & Beyer, J. E. (2005). Baltic cod recruitment—the impact of climate variability on key processes. *ICES Journal of marine science*, 62(7), 1408-1425.
- Laevastu, T., & Larkins, H. (1981). Marine fisheries ecosystem: its quantitative evaluation and management. Fish.
- Lehodey, P. (2005). *Reference Manual for the Spatial Ecosystem and Populations Dynamics Model – SEAPODYM*. WCPFC-SC1, ME IP- 1.



- Lehodey, P., Chai, F., Hampton, J. (2003). Modelling climate-related variability of tuna populations from a coupled ocean- biogeochemical-populations dynamics model. *Fisheries Oceanography* 12, 483–494.
- Lisovenko, L. A., & Andrianov, D. P. (1996). Reproductive biology of anchovy (*Engraulis encrasicolus ponticus* Alexandrov 1927) in the Black Sea. *Scientia Marina*, 60, 209-218.
- Longhurst, A.R., and Pauly, D. 1987. Ecology of tropical oceans. *Academic Press, London*,
- Majorova, A. & Tkacheva, K.S. (1960). Distribution and Conditions of Reproduction of Pelamid (*Sarda sarda*) in the Black Sea According to Data of the Period 1956-1957. *Rapp. Comm. Int. Mer Medit.*, 15(3), 17-23.
- Maury, O., Faugeras, B., Shin, Y.-J., Poggiale, J.-C., Ben Aria, T., Marsac, F., 2007. Modeling environmental effects on the size-structured energy flow through marine ecosystems. Part 1: the model. *Progress in Oceanography* 74, 479–499
- Mee, L.D. (2006). Reviving dead zones. *Sci. Am.* 295, 54–61.
- Morell, A., Shin, Y. J., Barrier, N., Travers-Trolet, M., Halouani, G., & Ernande, B. (2023). Bioen-OSMOSE: A bioenergetic marine ecosystem model with physiological response to temperature and oxygen. *Progress in Oceanography*, 103064.

- Moullec, F., Barrier, N., Drira, S., Guilhaumon, F., Marsaleix, P., Somot, S., ... & Shin, Y. J. (2019). An end-to-end model reveals losers and winners in a warming Mediterranean Sea. *Frontiers in Marine Science*, 6, 345.
- Murray, J. W., Jannasch, H. W., Honjo, S., Anderson, R. F., Reeburgh, W. S., Top, Z., ... & Izdar, E. (1989). Unexpected changes in the oxic/anoxic interface in the Black Sea. *Nature*, 338(6214), 411-413.
- Oguz, T. (2005). Black Sea ecosystem response to climatic teleconnections. *Oceanography*, 18(2), 122-133.
- Oguz, T. (2007). Nonlinear response of Black Sea pelagic fish stocks to over-exploitation. *Marine Ecology Progress Series*, 345, 211-228.
- Oguz, T., La Violette, P. E., & Unluata, U. (1992). The upper layer circulation of the Black Sea: Its variability as inferred from hydrographic and satellite observations. *Journal of Geophysical Research: Oceans*, 97(C8), 12569-12584.
- Oguz, T., Ducklow, H., Malanotte-Rizzoli, P., Tugrul, S., Nezlin, N. P., & Unluata, U. (1996). Simulation of annual plankton productivity cycle in the Black Sea by a one-dimensional physical-biological model. *Journal of Geophysical Research: Oceans*, 101(C7), 16585-16599.

- Oguz, T., Tuğrul, S., Kıdeys, A. E., Ediger, V., Kubilay, N. (2005). Physical and biogeochemical characteristics of the Black Sea. In A.R. Robinson & K.H. Brink (Eds.), *The Global Coastal Ocean-Interdisciplinary Regional Studies and Synthesis* (pp. 1331-1369). THE SEA Series, 14(33), Harvard University Press.
- Oguz, T., Dippner, J. W., & Kaymaz, Z. (2006). Climatic regulation of the Black Sea hydro-meteorological and ecological properties at interannual-to-decadal time scales. *Journal of Marine Systems*, 60(3-4), 235-254.
- Oguz, T., & Gilbert, D. (2007). Abrupt transitions of the top-down controlled Black Sea pelagic ecosystem during 1960–2000: evidence for regime-shifts under strong fishery exploitation and nutrient enrichment modulated by climate-induced variations. *Deep Sea Research Part I: Oceanographic Research Papers*, 54(2), 220-242.
- Oguz, T., Akoglu, E., & Salihoglu, B. (2012). Current state of overfishing and its regional differences in the Black Sea. *Ocean & Coastal management*, 58, 47-56.
- Oliveros-Ramos, R., & Shin, Y. J. (2016). Calibrar: an R package for fitting complex ecological models. *arXiv preprint arXiv:1603.03141*.
- Oliveros-Ramos, R., Verley, P., Echevin, V., & Shin, Y. J. (2017). A sequential approach to calibrate ecosystem models with multiple time series data. *Progress in Oceanography*, 151, 227-244.

- Ortega-García, A., & de-la-Gándara, F. (2008). Spawning of bonito, *Sarda sarda*, in captivity. *Centro Oceanográfico de Murcia*.
- Özdemir, S., Erdem, Y., Özdemir, Z. B., Erdem, E., & Hakan, A. K. S. U. (2018). Estimation of growth parameters and mortality rates of sprat (*Sprattus sprattus* L.) and anchovy (*Engraulis encrasicolus*, L.) captured in the Black Sea. *Turkish Journal of Maritime and Marine Sciences*, 4(2).
- Öztürk, B. (2013). Some remarks of Illegal, Unreported and Unregulated (IUU) fishing in Turkish part of the Black Sea. *Journal of Black Sea/Mediterranean Environment*, 19(2), 256-267.
- Pauly, D., Watson, R., & Alder, J. (2005). Global trends in world fisheries: impacts on marine ecosystems and food security. *Philosophical Transactions of the Royal Society B: Biological Sciences*, 360(1453), 5-12.
- Pennino, M. G., Coll, M., Albo-Puigserver, M., Fernández-Corredor, E., Steenbeek, J., Giráldez, A., ... & Bellido, J. M. (2020). Current and future influence of environmental factors on small pelagic fish distributions in the Northwestern Mediterranean Sea. *Frontiers in Marine Science*, 7, 566340.
- Perry, R. I., Cury, P., Brander, K., Jennings, S., Möllmann, C., & Planque, B. (2010). Sensitivity of marine systems to climate and fishing: concepts, issues and management responses. *Journal of Marine Systems*, 79(3-4), 427-435.

Pörtner, H. O., Karl, D. M., Boyd, P. W., Cheung, W., Lluich-Cota, S. E., Nojiri, Y., ... & Wittmann, A. C. (2014). Ocean systems. In *Climate change 2014: impacts, adaptation, and vulnerability. Part A: global and sectoral aspects. contribution of working group II to the fifth assessment report of the intergovernmental panel on climate change*, 411-484. Cambridge University Press.

Radu, G. & Maximov, V. (2011). State of the Black Sea Whiting (*Merlangius merlangus euxinus*) (Nordmann, 1840). GFCM Secretariat.

Raykov, V., Shlyakhov, V., Maximov, V., Radu, G., Staicu, I., Panayotova, M., ... & Bikarska, I. I. (2008). Limit and target reference points for rational exploitation of the turbot (*Psetta maxima* L.) and whiting (*Merlangius merlangus euxinus* Nordm.) in the western part of the Black Sea. In *VI Anniversary Conference of the Institute of Zoology*, 2, 305-315. Acta Zoologica Bulgarica.

Rose, K. A., Allen, J. I., Artioli, Y., Barange, M., Blackford, J., Carlotti, F., ... & Zhou, M. (2010). End-to-end models for the analysis of marine ecosystems: challenges, issues, and next steps. *Marine and Coastal Fisheries*, 2(1), 115-130.

Saglam, H., & Yıldız, I. (2019). Temporal and ontogenetic variation in the diet of three small pelagic fish in the Black Sea of Turkey. *Marine Biodiversity*, 49(4), 1799-1812.

- Satilmis, H. H., Sumer, C., Ozdemir, S., & Bayrakli, B. (2014). Length-weight relationships of the three most abundant pelagic fish species caught by mid-water trawls and purse seine in the Black Sea. *Cahiers de biologie marine*, 55(2), 259-265.
- Salihoglu, B., Arkin, S. S., Akoglu, E., & Fach, B. A. (2017). Evolution of future Black Sea fish stocks under changing environmental and climatic conditions. *Frontiers in Marine Science*, 4, 339.
- Sherman, K., & Adams, S. (Eds.). (2010). *Sustainable development of the World's large marine ecosystems during climate change: a commemorative volume to advance sustainable development on the occasion of the presentation of the 2010 Göteborg Award*. International Union for Conservation of Nature and Natural Resources.
- Shin, Y. J., & Cury, P. (2001). Exploring fish community dynamics through size-dependent trophic interactions using a spatialized individual-based model. *Aquatic Living Resources*, 14(2), 65-80.
- Shin, Y. J., & Cury, P. (2004). Using an individual-based model of fish assemblages to study the response of size spectra to changes in fishing. *Canadian Journal of Fisheries and Aquatic Sciences*, 61(3), 414-431.
- Stanev, E. V., Peneva, E., & Chtirkova, B. (2019). Climate change and regional ocean water mass disappearance: Case of the Black Sea. *Journal of Geophysical Research: Oceans*, 124, 4803–4819.

- STECF-15-16. 2015. Scientific, technical and economic committee for fisheries (STECF)—Black Sea assessments. Luxembourg: Publications Office of the European Union, 284.
- Stenseth, N. C., Mysterud, A., Ottersen, G., Hurrell, J. W., Chan, K. S., & Lima, M. (2002). Ecological effects of climate fluctuations. *Science*, 297(5585), 1292-1296.
- Sumaila, U.R. & Tai, T.C. (2020). End Overfishing and Increase the Resilience of the Ocean to Climate Change. *Front. Mar. Sci.* 7:523. doi: 10.3389/fmars.2020.00523
- Suzuki, N., Kondo, M., Gunes, E., Ozogun, M., & Ohno, A. (2001). Age and growth of turbot *Psetta maxima* in the Black Sea, Turkey. *Turkish Journal of Fisheries and Aquatic Sciences*, 1(2).
- Taylan, B., Gurkan, S., Taskavak, E., & Uncumusaoglu, A. A. (2018). A preliminary study of fecundity of whiting, *Merlangius merlangus euxinus* (Linnaeus, 1758) in coast of Tirebolu (Eastern Black Sea). *Turkish Journal of Agriculture-Food Science and Technology*, 6(3), 322-325.
- Taylor, K. E. (2001). Summarizing multiple aspects of model performance in a single diagram. *Journal of geophysical research: atmospheres*, 106(D7), 7183-7192.

- Travers, M., Shin, Y. J., Jennings, S., & Cury, P. (2007). Towards end-to-end models for investigating the effects of climate and fishing in marine ecosystems. *Progress in oceanography*, 75(4), 751-770.
- Travers, M., Shin, Y. J., Jennings, S., Machu, E., Huggett, J. A., Field, J. G., & Cury, P. M. (2009). Two-way coupling versus one-way forcing of plankton and fish models to predict ecosystem changes in the Benguela. *Ecological modelling*, 220(21), 3089-3099.
- Travers-Trolet, M., Shin, Y. J., Shannon, L. J., Moloney, C. L., & Field, J. G. (2014). Combined fishing and climate forcing in the southern Benguela upwelling ecosystem: an end-to-end modelling approach reveals dampened effects. *PloS one*, 9(4), e94286.
- Ulman, A., Bekisoglu, S., Zengin, M. A., Knudsen, S., Unal, V., Mathews, C., ... & Pauly, D. (2013). From bonito to anchovy: a reconstruction of Turkey's marine fisheries catches (1950-2010). *Mediterranean Marine Science*, 309-342.
- Ulman, A., Shlyakhov, V., Jatsenko, S., & Pauly, D. (2015). A reconstruction of the Ukraine's marine fisheries catches, 1950-2010. *Journal of Black Sea/Mediterranean Environment*, 21(2), 103-124.
- Zaitsev, Y., & Mamaev, V. (1997). Marine biological diversity in the Black Sea. A study of change and decline. GEF Black Sea Environmental Series, 3, 208.



Zengin, M. (2000). Türkiye'nin Doğu Karadeniz Kıyılarındaki Kalkan (*Scophthalmus maeoticus*, Pallas, 1811) Balığının Biyoekolojik Özellikleri ve Populasyon Parametreleri. Fen Bilimleri Enstitüsü, Bal. Tekn. Müh. Anabilim Dalı, Trabzon

Zengin, M., Gümüş, A., & Bostancı, D. (2006a). Age and growth of the Black Sea turbot, *Psetta maxima* (Linnaeus, 1758)(Pisces: Scophthalmidae), estimated by reading otoliths and by back-calculation. *Journal of Applied Ichthyology*, 22(5), 374-381.

Zengin, M. & Dinçer, A.C. (2006b). Distribution and seasonal movement of Atlantic bonito (*Sarda sarda*) populations in the Southern Black Sea coasts. *Turkish Journal of Fisheries and Aquatic Sciences*, 6(1), 57-62.



## APPENDICES

### A. OSMOSE-BS Parameters

Table A.1. References(1) for input parameters of OSMOSE-BS

Species	$L_{\infty}$	K	b	c	$t_0$
Anchovy	(Erdogan-Saglam & Saglam, 2013)	(Erdogan-Saglam & Saglam, 2013)	(Satilmis et al., 2014)	(Satilmis et al., 2014)	(Erdogan-Saglam & Saglam, 2013)
Sprat	(Avsar, 1995)	(Avsar, 1995)	(Satilmis et al., 2014)	(Satilmis et al., 2014)	(Avsar, 1995)
Horse mackerel	(Ceyhan et al., 2007)	(Aydin & Karadurmus, 2012)	(Satilmis et al., 2014)	(Satilmis et al., 2014)	(Ceyhan et al., 2007)
Red mullet	(Kasapoglu, 2018)	(Kasapoglu, 2018)	(Kasapoglu, 2018)	(Kasapoglu, 2018)	(Kasapoglu, 2018)
Whiting	(Kasapoglu, 2018)	(Kasapoglu, 2018)	(Kasapoglu, 2018)	(Kasapoglu, 2018)	(Kasapoglu, 2018)
Turbot	(Zengin et al., 2006a)	(Zengin et al., 2006a)	(STECF 15-16, 2015)	(STECF 15-16, 2015)	(Zengin et al., 2006a)
Bluefish		(Ceyhan et al., 2007)	(Kalayci et al., 2007)	(Kalayci et al., 2007)	(Ceyhan et al., 2007)
Bonito	(Ortega & Gandara, 2008)	(Kahraman et al., 2014)	(Kahraman et al., 2014)	(Kahraman et al., 2014)	(Kahraman et al., 2014)

Table A. 2. References (2) for input parameters for OSMOSE-BS

Species	$Ratio_{sex}$	$L_{mat}$	Life Span	$L_{max}$	$Egg_{size}$
Anchovy	(Erdoğan-Sağlam & Sağlam, 2013)	(Sağlam & Yıldız, 2019)	(STECF 15-16, 2015)	(Özdemir et al., 2018)	(Lisovenko & Andrianov, 1997)
Sprat	(Satılmış et al., 2014)	(Avsar & Bingel, 1994)	(Avsar, 1995)	(Özdemir et al., 2018)	(Avsar & Bingel, 1994)
Horse Mackerel	(Satılmış et al., 2014)	(Demirel & Yuksek, 2013)	(Aydın & Karadurmuş, 2012)	(Satılmış et al., 2014)	(Demirel & Yuksek, 2013)
Red Mullet	(Aydın & Karadurmuş, 2012)	(Genc, 2000)	(Aydın & Karadurmuş, 2012)	(Aydın & Karadurmuş, 2012)	(Aydın & Karadurmuş, 2013)
Whiting	(İşmen, 2002)	(Radu & Maximov, 2011)	(İşmen, 2002)	(İşmen, 2002)	(Taylan et al., 2018)
Turbot	(Genc, 2000)	(Eryılmaz & Dalyan, 2015)	(Suzuki et al., 2001)	(Avşar, 1999)	(Zengin, 2000)
Bluefish		(Ceyhan et al., 2007)	(Ceyhan et al., 2007)	(Ceyhan et al., 2007)	(IBB, 2020)
Bontio	(Kahraman et al., 2014)	(Kahraman et al., 2014)	(Majorova & Tkacheva, 1959)	(Kahraman et al., 2014)	(Ortega & Gandara, 2008)

Table A. 3. Parameters for calibration

	opt	min	max	phase
Zo accessibility rate to fish	0.5	0.1	1	1
Zm accessibility rate to fish	0.5	0.1	1	1
Dn accessibility rate to fish	0.5	0.05	1	1
$M_N$ of Anchovy	1	0.4	1.4	2
$M_N$ of Sprat	0.73	0.5	1.04	2
$M_N$ of Horse Mackerel	0.5	0.2	1.2	2
$M_N$ of Red Mullet	0.69	0.3	1	2
$M_N$ of Whiting	0.22	0.2	1	2
$M_N$ of Turbot	0.22	0.2	1	2
$M_N$ of Bluefish	0.44	0.3	1	2
$M_N$ of Bonito	0.64	0.4	1	2
$M_{out}$ of Bluefish	0.98	0.5	2	3
$M_{out}$ of Bluefish	0.42	0.4	2	3
$M_F$ of Anchovy	1.01	0.5	3	4
$M_F$ of Sprat	0.91	0.2	1.2	4
$M_F$ of Horse Mackerel	1.5	0.4	2	4
$M_F$ of Red Mullet	0.98	0.6	2	4
$M_F$ of Whiting	0.76	0.5	3	4
$M_F$ of Turbot	0.5	0.4	2	4

Table A. 3 (cont'd)

$M_F$ of Bluefish	0.98	0.5	2	4
$M_F$ of Bonito	0.42	0.3	2	4
Relative Fecundity of Anchovy	800	500	33000	5
Relative Fecundity of Sprat	277	28	3000	5
Relative Fecundity of Horse Mackerel	287	29	3000	5
Relative Fecundity of Red Mullet	168.25	17	3000	5
Relative Fecundity of Whiting	246.87	25	3000	5
Relative Fecundity of Turbot	611	61	6000	5
Relative Fecundity of Bluefish	305.4	31	3000	5
Relative Fecundity of Bontio	65	7	6500	5
$I_{max}$ of Anchovy	3.5	1	10	6
$I_{max}$ of Sprat	3.5	1	10	6
$I_{max}$ of Horse Mackerel	3.5	1	10	6
$I_{max}$ of Red Mullet	3.5	1	10	6
$I_{max}$ of Whiting	3.5	1	10	6
$I_{max}$ of Turbot	3.5	1	10	6
$I_{max}$ of Bluefish	3.5	1	10	6
$I_{max}$ of Bonito	3.5	1	10	6

---

Table A.4. Time series data used in model calibration and validation for biomass obtained from GFCM, (2022) for anchovy, and STECF 15-16, (2015) for others.

Year	Anchovy	Sprat	Horse Mackerel	Red mullet	Whiting	Turbot
2000	920862.3	427776	52099	6949	21235	5419
2001	901730.2	509464	52099	6026	14920	4794
2002	835918	481057	52099	5502	15838	4328
2003	632270.7	328386	52099	5922	12133	4196
2004	667055.7	275543	52099	8094	10092	4927
2005	684312.3	256567	51339	8322	10961	5473
2006	710245.2	269877	60306	9424	14892	6884
2007	709385.9	365323	76267	11096	18004	6579
2008	702800.1	417855	61894	9873	17440	6023
2009	540631.3	529054	50067	12565	15751	5497
2010	516482	329050	42704	15151	18413	4493
2011	513684.9	294278	54107	15394	13493	3730
2012	425764.8	229244	52691	14613	12979	3499
2013	528958.7	230559	36830	12501	13979	2466
2014	495180.6	277720	34789	11035	12024	1973

Table A.5. Time series data used in model calibration and validation for landings sourced from STECF 15-16, 2015; for bluefish and bonito (FAO, 2022)

Year	Anchovy	Sprat	Horse Mackerel	Whiting	Turbot	Red Mullet	Bluefish	Bonito
2000	270144	47994	16337	16955	2789	2487	7363	15039
2001	295760	63587	16911	9769	2557	1643	13573	12820
2002	344618	71944	9147	10369	1567	1731	23314	8392
2003	277893	47971	10257	7347	1122	1286	20728	8040
2004	315128	39481	9634	7490	1142	1303	18786	7679
2005	128223	46604	17602	6871	1400	1801	21157	93581
2006	226239	39923	13625	8008	1751	1501	9272	39529
2007	378046	38778	17886	11392	2259	1791	6973	7071
2008	255086	72766	20843	11162	2122	2089	4525	7549
2009	221660	91375	16489	9105	2078	2637	6538	6908
2010	248049	91594	13406	11987	1738	3952	5870	9991
2011	279300	120708	18559	8249	1659	3520	4343	10618
2012	171036	35025	24931	6346	1704	3491	8612	44346
2013	326130	27355	20114	8341	1522	2500	6095	16240
2014	157462	58380	12357	8819	1159	3895	10771	25214



Table A.6. Data used in model validation for mean sizes and their references.

Species	Size (cm)	Reference
Anchovy	10.64	(Kasapoglu, 2018)
Sprat	7.35	(Kasapoglu, 2018)
Horse Mackerel	12.3	(Kasapoglu, 2018)
Red Mullet	13.13	(Aydın & Karadurmuş, 2013)
Whiting	12.7	(Kasapoglu, 2018)
Turbot	35.62	(Özdemir et al., 2006)
Bluefish	20.34	(Bal et al., 2015)
Bonito	36.3	(Ateş et al., 2008)

## B. OSMOSE-BS Results

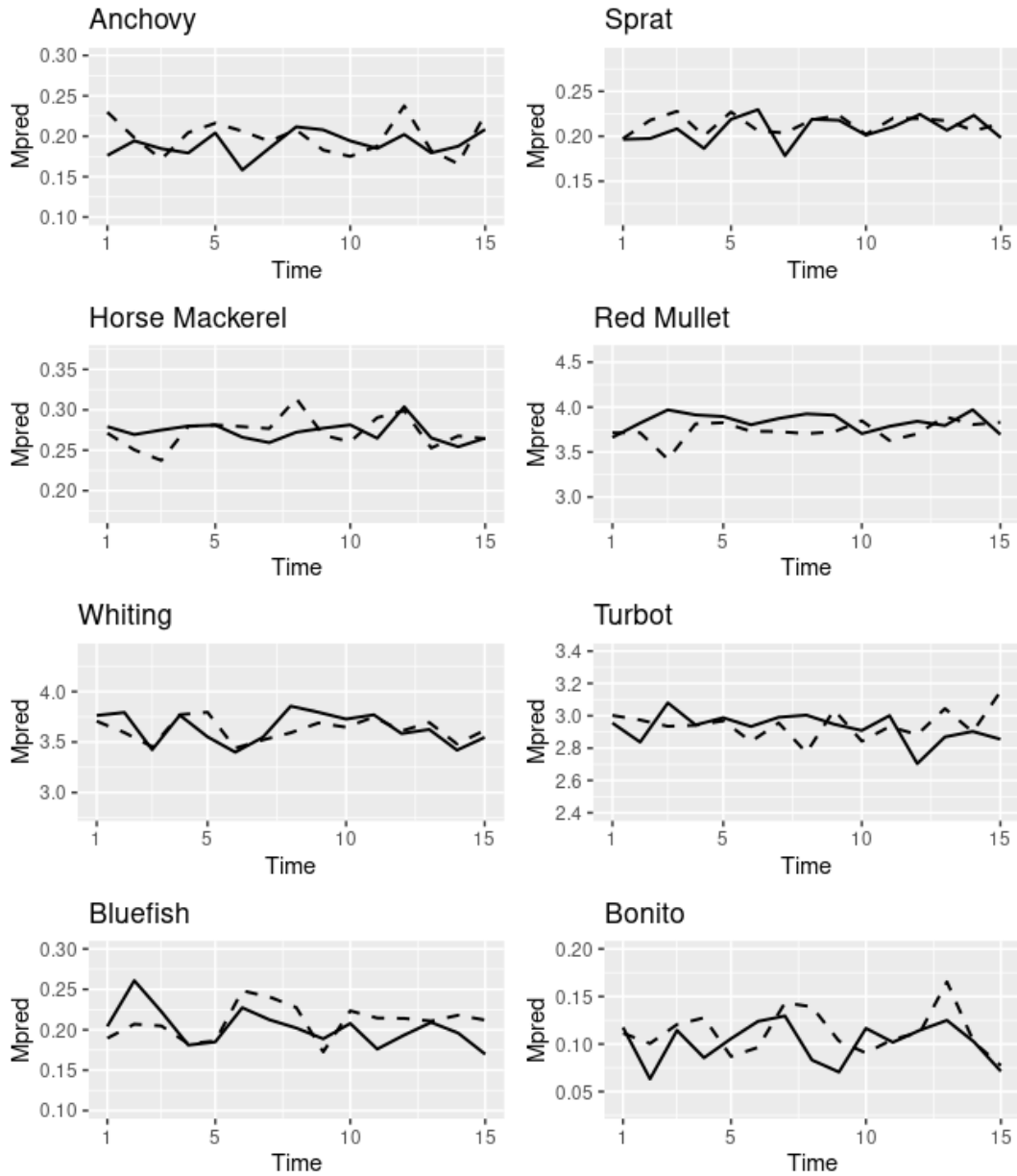


Figure B.1. Time series of the predation mortality for eight HTL species over a 15 year hindcast and forecast simulation. The solid line represents the forecast scenario (2086-2100), the dashed line represents the hindcast scenario (2000-2014).

Table B. 1. The mean predation mortality values predicted by OSMOSE-BS for the eight fish species over 15-years for both hindcast (2000-2014) and the future climate (2086-2100) scenarios.

Species	Hindcast	Forecast	<i>Percentage Change</i>
Anchovy	0.199	0.191	-4.3
Sprat	0.213	0.208	-2.6
Horse Mackerel	0.273	0.273	0
Red Mullet	3.739	3.838	2.6
Whiting	3.624	3.638	0.4
Turbot	2.945	2.928	-0.6
Bluefish	0.210	0.202	-3.7
Bonito	0.112	0.102	-9.3

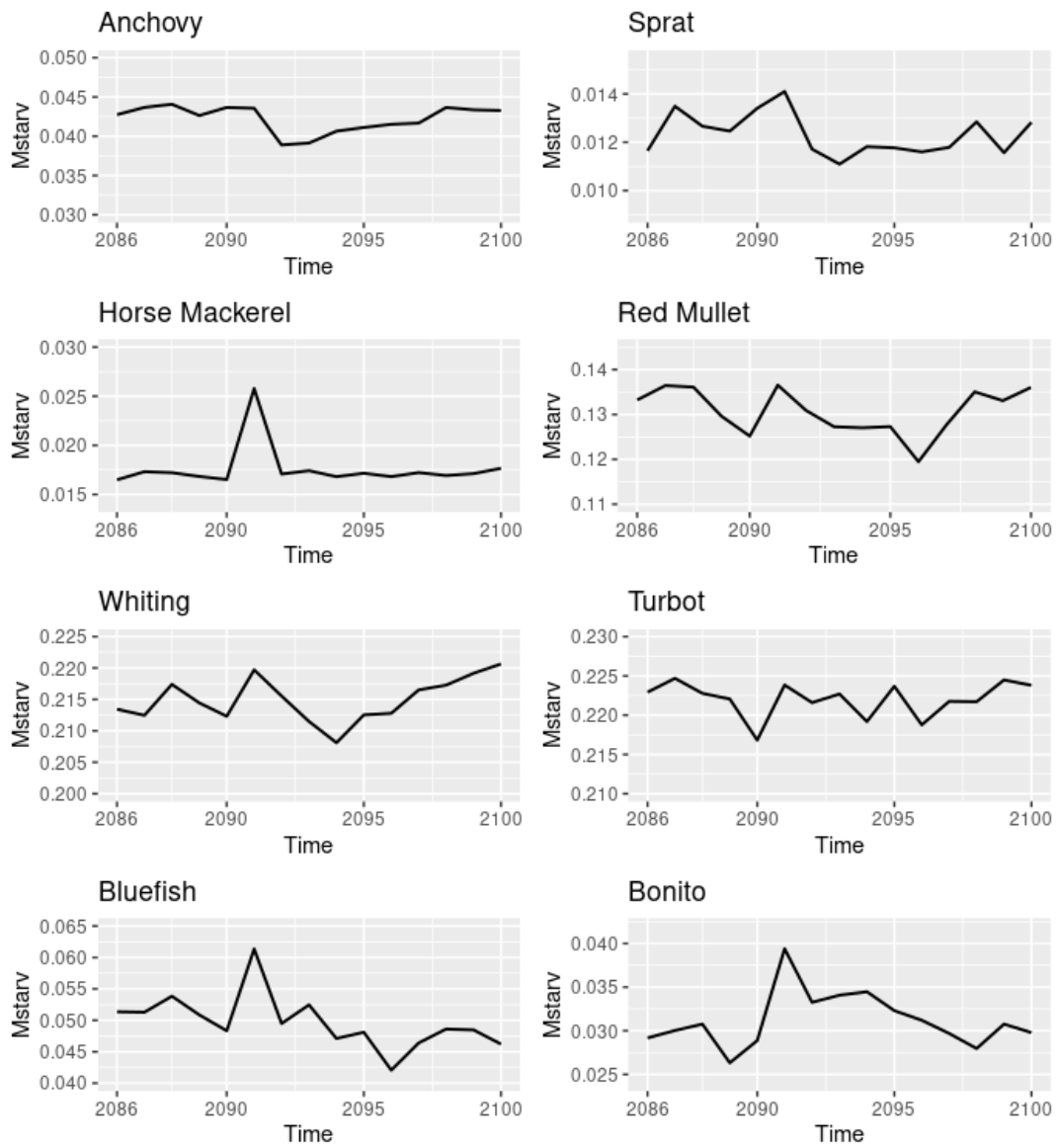


Figure B.2. Time series of starvation mortality for eight HTL species over a 15 year under future climate scenario (2086-2100).

### C. Lower Trophic Level Changes

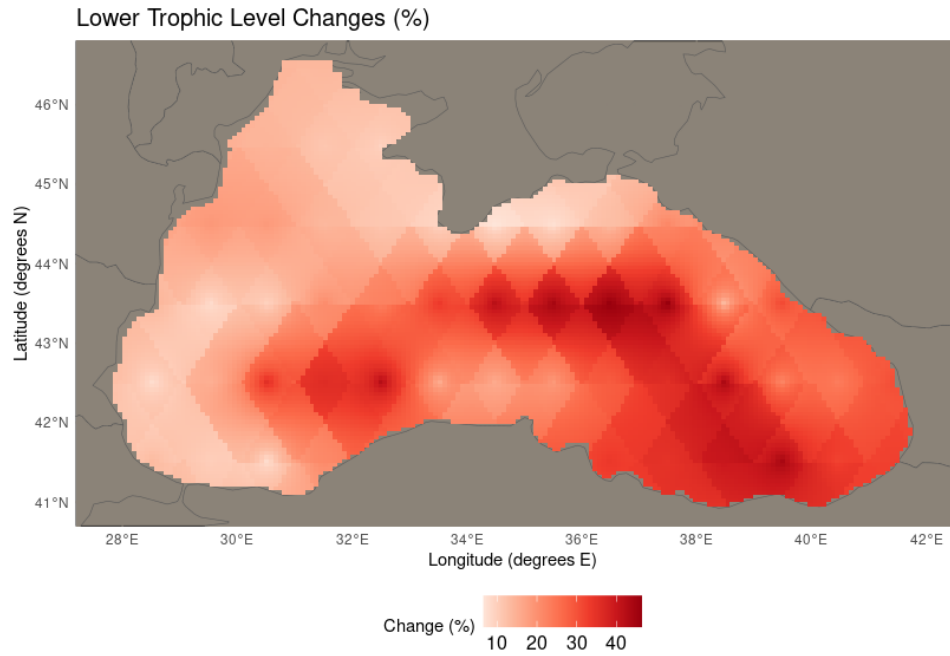


Figure C.1. The change in spatial distribution of total biomass of mesozooplankton, microzooplankton and detritus between the hindcast and forecast scenarios.